

A High-Order Local Projection Stabilization Method for Natural Convection Problems

Tomás Chacón Rebollo¹ · Macarena Gómez Mármol² · Frédéric Hecht³ · Samuele Rubino⁴ · Isabel Sánchez Muñoz⁵

Received: 26 October 2016 / Revised: 3 March 2017 / Accepted: 23 May 2017 / Published online: 5 June 2017
© Springer Science+Business Media New York 2017

Abstract In this paper, we propose a local projection stabilization (LPS) finite element method applied to numerically solve natural convection problems. This method replaces the projection-stabilized structure of standard LPS methods by an interpolation-stabilized structure, which only acts on the high frequencies components of the flow. This approach gives rise to a method which may be cast in the variational multi-scale framework, and constitutes a low-cost, accurate solver (of optimal error order) for incompressible flows, despite being only weakly consistent. Numerical simulations and results for the buoyancy-driven airflow in a square cavity with differentially heated side walls at high Rayleigh numbers (up to $Ra = 10^7$) are given and compared with benchmark solutions. Good accuracy is obtained with relatively coarse grids.

Keywords Boussinesq equations · Thermally coupled flows · Natural convection · LPS methods · Finite elements · Numerical analysis · High Rayleigh number flows

✉ Isabel Sánchez Muñoz
isanchez@us.es

Tomás Chacón Rebollo
chacon@us.es

Macarena Gómez Mármol
macarena@us.es

Frédéric Hecht
frederic.hecht@upmc.fr

Samuele Rubino
samuele.rubino@u-bordeaux.fr

¹ Departamento EDAN and IMUS, Universidad de Sevilla, Sevilla, Spain

² Departamento EDAN, Universidad de Sevilla, Sevilla, Spain

³ Laboratoire Jacques-Louis Lions, Université Paris VI, Paris, France

⁴ Laboratoire I2M, IPB (UMR CNRS 5295), Université de Bordeaux, Talence, France

⁵ Departamento Matemática Aplicada I, Universidad de Sevilla, Sevilla, Spain

1 Introduction

In the present paper, we discuss the application of finite element (FE) local projection stabilization (LPS) methods to natural convection problems. Natural convection occurs in many practical situations of real life, and the so-called Boussinesq approximation is generally employed to describe this physical phenomenon. The Boussinesq system models motion of buoyancy-driven incompressible fluid flows of relevant importance in nature (atmosphere, ocean dynamics) and industry (room ventilation, insulation with double-pane windows, cooling of nuclear reactors, material processing, etc.).

From the computational point of view, the Boussinesq system presents severe problems for large Rayleigh numbers. It is well known that its steady solution is unique only under some restrictions on the Rayleigh and Prandtl numbers. Uniqueness is lost for very high Rayleigh numbers [47], at which the solution bifurcates due to the instability of the basic flow that leads to an oscillating flow pattern (transition to thermal turbulence). Standard Galerkin FE methods for natural convection problems usually yield inaccurate approximate solutions (unless using very fine unpractical grids) at large Rayleigh numbers, due to the dominant convection inside layers that generates spurious instabilities [33]. Remaining in the context of FE methods, a more coherent formulation to properly reproduce buoyancy-driven convection-dominated flows should take into account additional stabilization techniques [48] in order to represent a viable numerical method.

We mainly focus here on a high-order LPS method (Cf. [19]), which constitutes a low-cost, accurate solver for incompressible flows, despite being only weakly consistent since it does not involve the full residual. It differs from the standard LPS methods (Cf. [15,39]) because it uses continuous buffer functions, it does not need enriched FE spaces, it does not need element-wise projections satisfying suitable orthogonality properties, and it does not need multiple meshes. An interpolant-stabilized structure of Scott–Zhang-type replaces the projection-stabilized structure of standard LPS methods. This high-order stabilization procedure by using a Scott–Zhang-like interpolation operator has been successfully applied to the Oseen problem (Cf. [19]). Moreover, it has been extended to the evolution NSE (Cf. [21]) and the primitive equations of the ocean (Cf. [24]), and recently shown by numerical experiments that, since this method is only approximately consistent, the addition of a multi-scale Smagorinsky term to the high-order stabilization scheme can help to counter-balance the accumulation of sub-grid energy due to its diffusive nature, providing slight additional accuracy (Cf. [23,49]).

LPS schemes were originally proposed for the Stokes problem [8], and then successfully extended to transport problems (Cf. [3,6,9,38,45,48]). They allow to circumvent the discrete inf–sup condition and to use equal order interpolation for velocity and pressure and they also provide stabilization of convection-dominant effects and improvement of mass conservation. Different variants of LPS methods have been investigated during the recent years for incompressible flow problems. The main common interesting feature is that, thanks to projection, the symmetric stabilization terms only act on the small scales of the flow as sub-grid viscosities, thus ensuring a higher accuracy with respect to more classical stabilization procedures, such as penalty-stabilized methods (Cf. [18]). This also guarantees a self-adapting high accuracy in laminar regions of a turbulent flow, which turns to be of overall optimal high accuracy if the flow is fully laminar, and allows to obtain an asymptotic energy balance for smooth flows (Cf. [1]). Moreover, an important advantage of their term-by-term structure is that the projection can be easily treated as implicit, without having all the residual terms coupled, as for more complex residual-based methods (Cf. [7,29]). For a detailed description of different variants of LPS schemes, we refer to [34,39,52].

The numerical analysis of LPS methods is well-understood for the Oseen problem (Cf. [15, 16, 30, 44, 46]). This analysis has been recently extended to the time-dependent incompressible Navier–Stokes equations (NSE) in [4, 17], and also in [1, 21, 22] for the term-by-term version of the method considered in the present paper when just applied to NSE. Also, some numerical analysis and numerical results for steady and time-dependent natural convection problems can be found in the literature [10, 13, 14]. In [26–28, 41, 54], sub-grid scale modeling for (turbulent) temperature dependent flow is considered. However, when stabilized methods are used, the existent numerical analysis only concerns the study of dissipative stabilization terms acting as sub-grid viscosities, and the analysis of non-symmetric crossed stabilization terms coming from the coupling of energy and momentum in Navier–Stokes equations is not yet available, to the best of our knowledge. The present paper aims to provide such a technical analysis, which cannot be found in the literature so far, up to the authors knowledge.

The main contribution of this work is thus to extend the formulation and the numerical analysis introduced in [1] for NSE to non-isothermal incompressible flows using the Boussinesq approximation, in which the unknowns, velocity, pressure and temperature, are strongly coupled. Also, to discuss some implementations aspects of the extended formulation. This latter is mathematically derived using the variational multi-scale (VMS) formalism [2, 25, 37]. The basic idea is to split the unknowns, velocity, pressure and temperature, into their FE component (resolved scales of the flow) and a sub-grid scale component, hereafter referred to as sub-scale. This procedure makes apparent the presence of interactions between resolved scales and sub-scales that correspond to classical dissipative stabilization terms. Also, of crossed velocity-temperature interactions due to the coupling of heat and momentum equations, which in principle could not be neglected a-priori due to the relevant buoyancy interaction at all scale ranges introduced by the Boussinesq model, responsible for natural convection.

We extend the numerical analysis of [1] for NSE, deriving standard $L^\infty(\mathbf{L}^2) \cap L^2(\mathbf{H}^1)$ stability estimates for velocity and temperature in the evolutionary case. The new crossed stabilization terms due to velocity-temperature interactions are controlled using on one hand the L^2 estimates of velocity and temperature coming from their time derivative, and on the other hand the estimates of the dissipative stabilization terms. The obtained stability estimates are sufficient to pass to the weak limit in the evolution problem.

The paper is organized as follows: In Sect. 2, we introduce the model problem for time-dependent natural convection and its continuous variational formulation. In Sect. 3, we derive the proposed LPS approximation of the governing Boussinesq equations, and we state its main properties. Section 4 is devoted to the numerical analysis (stability and convergence) of the arising discrete stabilized FE scheme. In Sect. 5, we present numerical tests for the 2D motion of a fluid in a square cavity whose vertical walls are maintained at different temperatures. Numerical results are compared with reference solutions to show the potential of the proposed method for simulating high Rayleigh number flows on relatively coarse grids. Section 6 states the main conclusions of the paper.

2 Time-Dependent Boussinesq Equations: Continuous Problem and Variational Formulation

We introduce an initial–boundary value problem (IBVP) for the time-dependent Boussinesq equations to solve natural convection problems.

Let $\Omega \in \mathbb{R}^d$, with $d = 2$ or 3 , be the bounded polyhedral computational domain in which the flow takes place during the time interval $[0, T]$. Let $\Gamma = \partial\Omega$ be its Lipschitz-

continuous boundary that we suppose decomposed into two disjoint parts, $\Gamma = \Gamma_D \cup \Gamma_N$. Let us assume the fluid viscous, incompressible, Newtonian and Boussinesq-approximated. Thus, the IBVP to be considered consists in finding a velocity field $\mathbf{u} : \Omega \times (0, T) \rightarrow \mathbb{R}^d$, a pressure $p : \Omega \times (0, T) \rightarrow \mathbb{R}$, and a temperature $\theta : \Omega \times (0, T) \rightarrow \mathbb{R}$ such that:

$$\begin{cases} \partial_t \mathbf{u} + \mathbf{u} \cdot \nabla \mathbf{u} - Pr \Delta \mathbf{u} + \nabla p - Pr Ra \theta \mathbf{e}_d = \mathbf{f} & \text{in } \Omega \times (0, T) \\ \nabla \cdot \mathbf{u} = 0 & \text{in } \Omega \times (0, T) \\ \partial_t \theta + \mathbf{u} \cdot \nabla \theta - \Delta \theta = Q & \text{in } \Omega \times (0, T) \\ \mathbf{u}(\mathbf{x}, 0) = \mathbf{u}_0(\mathbf{x}) & \text{in } \Omega \\ \theta(\mathbf{x}) = \theta_0(\mathbf{x}) & \text{in } \Omega \\ \mathbf{u} = \mathbf{0} & \text{on } \Gamma \times (0, T) \\ \theta = \theta_D & \text{on } \Gamma_D \times (0, T) \\ \nabla \theta \cdot \mathbf{n} = 0 & \text{on } \Gamma_N \times (0, T) \end{cases} \tag{1}$$

Here, Pr and Ra are positive dimensionless numbers, respectively, the Prandtl and Rayleigh numbers, and \mathbf{e}_d is the last vector of the canonical basis of \mathbb{R}^d . The data are the external body forces field \mathbf{f} , the heat source term Q , the initial velocity field \mathbf{u}_0 , the initial temperature θ_0 , and a given temperature θ_D over the boundary Γ_D . In system (1), the governing equations of fluid flow corresponds respectively to momentum, mass, and energy conservation, together with initial and boundary conditions for the velocity field and the temperature (Cf. [40]). The Prandtl number is defined as:

$$Pr := \frac{\nu_0}{k_0},$$

with ν_0 a reference kinematic viscosity and k_0 a reference thermal conductivity. The Rayleigh number is defined as:

$$Ra := \frac{g \alpha_0 |\theta_1 - \theta_0| L^3}{k_0 \nu_0},$$

with g the gravitational acceleration, α_0 the thermal expansion coefficient, θ_1 and θ_0 references temperatures, and L a characteristic length. The Rayleigh number is associated with the heat transfer within the fluid and it measures the ratio between buoyancy and viscous forces. When the Rayleigh number is below a critical value, heat transfer is primarily in the form of conduction, but when it exceeds this critical value, heat transfer is primarily in the form of convection. Moreover, in the last case, if the Rayleigh number exceeds certain threshold the flow is unstable. This instability, called Rayleigh–Bénard instability, appears when there is a coupling between the dynamic field and the thermal field (Cf. [50]).

To define the weak formulation of problem (1), we introduce some useful notations for spaces. We consider the Sobolev spaces $L^p(\Omega)$, $W^{m,p}(\Omega)$, with $m \in \mathbb{N}$ and $1 \leq p \leq \infty$, and $H^s(\Omega)$, with $s \in \mathbb{R}$. When they appear as sub-index, they shall be denoted by L^p , $W^{m,p}$ and H^s , respectively. In the same way, the vector-valued Sobolev spaces shall be denoted by \mathbf{L}^p , $\mathbf{W}^{m,p}$ and \mathbf{H}^s , respectively. Also, the parabolic Bochner function spaces $L^p(0, T; X)$ and $L^p(0, T; \mathbf{X})$, where X or \mathbf{X} stands for a scalar or vector-valued Sobolev space, shall be denoted by $L^p(X)$ and $L^p(\mathbf{X})$, respectively.

We shall consider homogeneous Dirichlet data for the temperature, $\theta_D = 0$. As is standard, this condition may be achieved by using a convenient lifting of θ_D . Let us define the velocity and temperature spaces:

$$\begin{aligned} \mathbf{H}_0^1(\Omega) &= H_0^1(\Omega)^d = \left\{ \mathbf{v} \in H^1(\Omega)^d \text{ such that } \mathbf{v} = \mathbf{0} \text{ on } \Gamma \right\}, \\ H_D^1(\Omega) &= \{ z \in H^1(\Omega) \text{ such that } z = 0 \text{ on } \Gamma_D \}. \end{aligned}$$

These spaces are closed linear subspaces of $H^1(\Omega)^d$ and $H^1(\Omega)$, respectively, and thus Hilbert spaces endowed with the H^1 -norm. Thanks to Korn’s inequality (Cf. [36]), this norm is equivalent on $\mathbf{H}_0^1(\Omega)$ to the norm $\|v\|_{\mathbf{H}_0^1} = \|\nabla v\|_{L^2}$ and similarly, on $H_D^1(\Omega)$ to the norm $\|z\|_{H_D^1} = \|\nabla z\|_{L^2}$. We introduce the tensor space $\mathbf{X} = \mathbf{H}_0^1(\Omega) \times H_D^1(\Omega)$ endowed with the euclidean norm:

$$\|V\|_{\mathbf{X}}^2 = \|\nabla v\|_{L^2}^2 + \|\nabla z\|_{L^2}^2, \quad \forall V = (v, z) \in \mathbf{X},$$

and we denote by \mathbf{X}' its dual space. Also, we define the pressure space:

$$M = L_0^2(\Omega) = \left\{ q \in L^2(\Omega) \text{ such that } \int_{\Omega} q \, dx = 0 \right\}.$$

We consider the following variational formulation of (1):

Given $\mathbf{F} = (\mathbf{f}, Q) \in L^2(0, T; \mathbf{X}')$ and $U_0 = (\mathbf{u}_0, \theta_0) \in L^2(\Omega)^{d+1}$, find $\mathbf{U} = (\mathbf{u}, \theta) \in L^2(0, T; \mathbf{X})$ and $P \in L^2(0, T; M)$ such that:

$$\left\{ \begin{array}{l} - \int_0^T (\mathbf{U}(t), \mathbf{V}) \varphi'(t) \, dt - (\mathbf{U}_0, \mathbf{V}) \varphi(0) \\ + \int_0^T [b(\mathbf{u}(t); \mathbf{U}(t), \mathbf{V}) + a(\mathbf{U}(t), \mathbf{V}) + c(\mathbf{U}(t), \mathbf{V})] \varphi(t) \, dt \\ + \int_0^T (P(t), \nabla \cdot \mathbf{v}) \varphi'(t) \, dt + \int_0^T (\nabla \cdot \mathbf{u}(t), q) \varphi(t) \, dt = \int_0^T (\mathbf{F}(t), \mathbf{V}) \varphi(t) \, dt, \\ \forall \mathbf{V} = (\mathbf{v}, z) \in \mathbf{X}, \forall q \in M, \forall \varphi \in \mathcal{D}([0, T]) \text{ such that } \varphi(T) = 0. \end{array} \right. \tag{2}$$

Here, (\cdot, \cdot) denotes the L^2 scalar product, either for scalar or vector functions, $\langle \cdot, \cdot \rangle$ stands for the duality pairing between \mathbf{X}' and \mathbf{X} , and the forms b, a and c are respectively given by:

$$b(\mathbf{w}; \mathbf{U}, \mathbf{V}) = \frac{1}{2} [(\mathbf{w} \cdot \nabla \mathbf{u}, \mathbf{v}) - (\mathbf{w} \cdot \nabla \mathbf{v}, \mathbf{u}) + (\mathbf{w} \cdot \nabla \theta, z) - (\mathbf{w} \cdot \nabla z, \theta)], \tag{3}$$

$$a(\mathbf{U}, \mathbf{V}) = r (\nabla \mathbf{u}, \nabla \mathbf{v}) + s (\nabla \theta, \nabla z), \tag{4}$$

$$c(\mathbf{U}, \mathbf{V}) = -\lambda (\theta, v_d), \tag{5}$$

for any $\mathbf{U}, \mathbf{V} \in \mathbf{X}, \mathbf{w} \in \mathbf{H}_0^1(\Omega)$. In the natural convection case that represents model (1), $r = Pr, s = 1$ and $\lambda = Pr Ra$, but the same structure covers others convection cases. For example, for mixed convection, $r = Re^{-1}, s = (Re Pr)^{-1}$ and $\lambda = Ra Re^{-1}$, with Re the Reynolds number. So, the numerical analysis realized in Sect. 4 is valid for different convection cases. Note that the linear forms b, a and c are continuous, and also that $b(\mathbf{w}; \mathbf{U}, \mathbf{U}) = 0$ for all $\mathbf{U} \in \mathbf{X}, \mathbf{w} \in \mathbf{H}_0^1(\Omega)$. The physical pressure is the time derivative of the unknown $P : p = \partial_t P \in H^{-1}(M) = H_0^1(0, T; M)'$. The interest of considering P as unknown instead of p is that there are high technical difficulties to obtain uniform bounds for the discrete pressures in a Banach space of space-time functions (see [25], Remark 10.2), while we shall obtain uniform bounds in the Banach space $L^\infty(L^2)$ for the numerical approximation of P (see estimate (29) of Theorem 4.7). It is known that for domains which satisfy the cone condition, as bounded polyhedral domains, $P \in L^\infty(L^2)$, e.g., see [32, Remark 2.5]. We notice, however, that for practical computations one would approximate the physical pressure p , and P is introduced just for the numerical analysis.

3 A High-Order LPS Discretization

In order to describe the discretization of problem (2), we consider a family of affine-equivalent, conforming, and regular triangulations of $\bar{\Omega}$ formed by simplicial elements, $\{\mathcal{T}_h\}_{h>0}$, where the parameter h denotes the largest diameter of the elements of \mathcal{T}_h .

Given an integer $l \geq 0$ and an element $K \in \mathcal{T}_h$, we denote by $\mathbb{P}_l(K)$ the space of Lagrange polynomials of degree less than, or equal to l , defined on K , and we define the following FE spaces:

$$\begin{aligned} V_h^l &= \{v_h \in C^0(\bar{\Omega}) \text{ such that } v_h|_K \in \mathbb{P}_l(K), \forall K \in \mathcal{T}_h\}, \\ \mathcal{U}_h &= (V_h^l \cap H_0^1(\Omega))^d, \quad \Theta_h = V_h^m \cap H_D^1(\Omega), \quad \mathbf{X}_h = \mathcal{U}_h \times \Theta_h \subset \mathbf{X}, \\ M_h &= V_h^n \cap M. \end{aligned} \tag{6}$$

To introduce a two-scales VMS model, we decompose the unknowns spaces \mathbf{X} and M as:

$$\mathbf{X} = \mathbf{X}_h \oplus \mathbf{X}', \quad M = M_h \oplus M',$$

where \mathbf{X}_h and M_h are the large-scales spaces for velocity-temperature and pressure, and \mathbf{X}' and M' are the small-scales complementary spaces. We shall assume that these two spaces are L^2 -orthogonal. Let us consider the corresponding decomposition of a solution $(\mathbf{U}(t), p(t))$ of (2) and the test functions (\mathbf{V}, q) :

$$(\mathbf{U}(t), p(t)) = (\mathbf{U}_h(t), p_h(t)) + (\mathbf{U}'(t), p'(t)), \quad (\mathbf{V}, q) = (\mathbf{V}_h, q_h) + (\mathbf{V}', q').$$

Then, the pairs $(\mathbf{U}_h(t), p_h(t))$ and $(\mathbf{U}'(t), p'(t))$ satisfy the following two coupled problems in $\mathcal{D}'(0, T)$ (for simplicity of notation, we do not explicit the dependence of these functions upon t):

$$(\partial_t \mathbf{U}_h, \mathbf{V}_h) + A(\mathbf{u}; (\mathbf{U}_h, p_h), (\mathbf{V}_h, q_h)) = \langle R(\mathbf{u}; \mathbf{U}', p'), (\mathbf{V}_h, q_h) \rangle, \tag{7}$$

for all $(\mathbf{V}_h, q_h) \in \mathbf{X}_h \times M_h$, and:

$$(\partial_t \mathbf{U}', \mathbf{V}') + A(\mathbf{u}; (\mathbf{U}', p'), (\mathbf{V}', q')) = \langle R(\mathbf{u}; \mathbf{U}_h, p_h), (\mathbf{V}', q') \rangle, \tag{8}$$

for all $(\mathbf{V}', q') \in \mathbf{X}' \times M'$, where:

$$A(\mathbf{w}; (\mathbf{U}, p), (\mathbf{V}, q)) = b(\mathbf{w}; \mathbf{U}, \mathbf{V}) + a(\mathbf{U}, \mathbf{V}) + c(\mathbf{U}, \mathbf{V}) - (p, \nabla \cdot \mathbf{v}) + (\nabla \cdot \mathbf{u}, q),$$

$R(\mathbf{w}; \mathbf{U}, p) = \begin{pmatrix} \mathbf{F} \\ 0 \end{pmatrix} - \begin{pmatrix} \partial_t \mathbf{U} \\ 0 \end{pmatrix} - \mathcal{L}_{\mathbf{w}}(\mathbf{U}, p)$ is the residual associated to the Eq. (1) and $\mathcal{L}_{\mathbf{w}}$ is the linear operator associated to the form $A(\mathbf{w}; \cdot, \cdot)$:

$$\mathcal{L}_{\mathbf{w}}(\mathbf{U}, p) = \begin{pmatrix} \mathbf{w} \cdot \nabla \mathbf{u} - r \Delta \mathbf{u} + \nabla p - \lambda \theta \mathbf{e}_d \\ \mathbf{w} \cdot \nabla \theta - s \Delta \theta \\ \nabla \cdot \mathbf{u} \end{pmatrix}.$$

Problem (8) has to be understood as a problem for the small-scales of the solution, (\mathbf{U}', p') , which are driven by the residual associated to the large-scales (\mathbf{U}_h, p_h) . Hence, supposing that the small-scales are quasi-static, this problem is approximately solved following the orthogonal sub-scales approach, that we omit for brevity (Cf. [2]) and its solution is represented in terms of the large-scales:

$$(\mathbf{U}', p') \approx \tau \Pi_h^*(R(\mathbf{u}_h; \mathbf{U}_h, p_h)), \tag{9}$$

where τ is a piecewise constant matrix that takes the value τ_K on any $K \in \mathcal{T}_h$ and $\Pi_h^* = I - \Pi_h$, with Π_h (in principle) the L^2 orthogonal projection on $X_h \times M_h$. Here we will assume that, in general, Π_h is some stable projection or interpolation operator on $X_h \times M_h$.

Problem (7) is regarded as a problem for the large-scales where the small-scales act as a parameter. Indeed, since $\partial_t U'$ is orthogonal to X_h , problem (7) can be rewritten as:

$$(\partial_t U_h, V_h) + A(u; (U_h, p_h), (V_h, q_h)) + \langle \mathcal{L}_u^* (V_h, q_h), (U', p') \rangle = \langle F, V_h \rangle, \quad (10)$$

for all $(V_h, q_h) \in X_h \times M_h$. Next, we approximate the convection velocity in \mathcal{L}_u^* by u_h and incorporate the approximation (9) in (10), considering that the force vector F belonging to the FE space (or being approximated by an element of this space). Then, we obtain the following VMS method to compute (U_h, p_h) :

$$\begin{aligned} & (\partial_t U_h, V_h) + A(u_h; (U_h, p_h), (V_h, q_h)) - (\Pi_h^*(\mathcal{L}_{u_h}^* (V_h, q_h)), \Pi_h^*(\mathcal{L}_{u_h}(U_h, p_h)))_{\tau} \\ & = \langle F, V_h \rangle, \quad \text{for all } (V_h, q_h) \in X_h \times M_h, \end{aligned} \quad (11)$$

where $(\cdot, \cdot)_{\tau}$ stands for the scalar product defined by:

$$(\varphi, \psi)_{\tau} = \sum_{K \in \mathcal{T}_h} \tau_K (\varphi, \psi)_{L^2(K)}, \quad \text{for all } \varphi, \psi \in L^2(\Omega)^{d+2}. \quad (12)$$

The spatial discretization that we propose to solve problem (2) is a penalty stabilized method based in method (11), where we neglect second order derivatives of FE functions within element interiors in:

$$-(\Pi_h^*(\mathcal{L}_{U_h}^* (V_h, q_h)), \Pi_h^*(\mathcal{L}_{U_h}(U_h, p_h)))_{\tau}.$$

This way leads to a method where we retain all the sub-grid dissipative interaction terms that correspond to classical stabilization terms but also all the sub-grid crossed velocity-pressure-temperature interaction terms due to the coupling of the heat and the momentum flow. These terms model the buoyancy effects from the small to the large scales. More concretely, we add to the standard Galerkin discretization the term $S_h(u_h; (U_h, p_h), (V_h, q_h))$ defined by:

$$\begin{aligned} S_h(w_h; (U_h, p_h), (V_h, q_h)) &= S_h^{mom}(w_h; (U_h, p_h), (V_h, q_h)) + S_h^{conv}(w_h; U_h, V_h) \\ &+ S_h^{div}(U_h, V_h) + S_h^{buo}(w_h; (U_h, p_h), (V_h, q_h)), \end{aligned} \quad (13)$$

where:

$$\begin{aligned} S_h^{mom}(w_h; (U_h, p_h), (V_h, q_h)) &= (\Pi_{h,1}^*(w_h \cdot \nabla v_h + \nabla q_h), \Pi_{h,1}^*(w_h \cdot \nabla u_h + \nabla p_h))_{\tau_1}, \\ S_h^{conv}(w_h, U_h, V_h) &= (\Pi_{h,2}^*(w_h \cdot \nabla z_h), \Pi_{h,2}^*(w_h \cdot \nabla \theta_h))_{\tau_2}, \\ S_h^{div}(U_h, V_h) &= (\Pi_{h,3}^*(\nabla \cdot v_h), \Pi_{h,3}^*(\nabla \cdot u_h))_{\tau_3}, \\ S_h^{buo}(w_h; (U_h, p_h), (V_h, q_h)) &= -\lambda (\Pi_{h,1}^*(w_h \cdot \nabla v_{hd} + \partial_d q_h), \Pi_{h,1}^*(\theta_h))_{\tau_1} \\ &+ \lambda (\Pi_{h,2}^*(v_{hd}), \Pi_{h,2}^*(w_h \cdot \nabla \theta_h))_{\tau_2}, \end{aligned}$$

for any $U_h = (u_h, \theta_h)$, $V_h = (v_h, z_h) \in X_h$, $w \in \mathbf{H}_0^1(\Omega)$ and $p_h, q_h \in M_h$.

Here, we consider Π_h some stable projection or interpolation operator from $L^2(\Omega)^{d+2}$ on $V_h^{l-1} \times V_h^{m-1} \times V_h^{n-1}$, and we denote by $\Pi_{h,1}$, $\Pi_{h,2}$ and $\Pi_{h,3}$ the components of this operator on V_h^{l-1} , V_h^{m-1} and V_h^{n-1} , respectively. This structure of the operator Π_h allows to

get optimal order, as it has been proved for the Oseen equations in [19], where this high-order method was introduced, and also for the unsteady Navier–Stokes equations in [1].

Also, we are considering in (12) the piecewise constant matrix τ that on each $K \in \mathcal{T}_h$ takes the value:

$$\tau_K = \left(\begin{array}{c|c|c} \tau_{K,1} I_d & 0 & 0 \\ \hline 0 & \tau_{K,2} & 0 \\ \hline 0 & 0 & \tau_{K,3} \end{array} \right),$$

where $\tau_{1,K}$, $\tau_{2,K}$ and $\tau_{3,K}$ are the stabilization coefficients. So:

$$\begin{aligned} (\varphi, \psi)_\tau &= \sum_{K \in \mathcal{T}_h} \tau_{K,1} (\varphi_1, \psi_1)_{L^2(K)^d} + \sum_{K \in \mathcal{T}_h} \tau_{K,2} (\varphi_2, \psi_2)_{L^2(K)} + \sum_{K \in \mathcal{T}_h} \tau_{K,3} (\varphi_3, \psi_3)_{L^2(K)} \\ &:= (\varphi_1, \psi_1)_{\tau_1} + (\varphi_2, \psi_2)_{\tau_2} + (\varphi_3, \psi_3)_{\tau_3}. \end{aligned}$$

We will denote $\| \cdot \|_\tau$, where τ denotes either τ_1 , τ_2 or τ_3 , the norm associated to the scalar products $(\cdot, \cdot)_\tau$, and define the space endowed with this norm:

$$L^2_\tau(\Omega) = \{ \varphi \in L^2(\Omega) \text{ such that } \|\varphi\|_\tau < +\infty \},$$

and similarly for vector functions.

The terms S_h^{mom} , S_h^{conv} and S_h^{div} enable to stabilize the interaction between velocity convection and pressure gradient, the temperature convection and the divergence of velocity, respectively (Cf. [1, 19, 21]). In this work, we aim to investigate the effect of the terms due to the buoyancy force.

Remark 3.1 Several authors have studied the links between residual LPS methods and VMS strategies. Braack and Burman established a connection between LPS and VMS modeling in [15], in the context of a three-scales VMS formulation of Navier–Stokes equations. In this work, LPS is used to construct eddy diffusion terms that vanish on the resolved large scales. Also, Barrenechea and Valentin design consistent LPS methods in [5], starting from a VMS formulation: An enriched Petrov–Galerkin formulation for the Stokes problem, in which velocity and pressure finite element spaces are enhanced with solutions of residual-based local problems. Then the static condensation procedure is applied to build the method. The resulting method does not need the use of a macro-element grid structure and is parameter-free.

Here we follow a different approach: We construct at first the two-level VMS formulation of Boussinesq equations, and retain the sub-grid diffusive terms, in addition to those generated by buoyancy interactions, to design the LPS discretization that we consider.

To introduce the discretization in time, we consider a positive integer number N and define $\Delta t = T/N$ and $t_n = n\Delta t$ for $n = 0, 1, \dots, N$. Then, we get a fully discrete scheme choosing a semi-implicit Euler method in time, where the discretization is semi-implicit for the convection terms, explicit for the term due to buoyancy (5), and implicit for the remaining terms.

We propose the following method to compute the approximations $U_h^n = (\mathbf{u}_h^n, \theta_h^n)$ and p_h^n of $U(\cdot, t_n) = (\mathbf{u}(\cdot, t_n), \theta(\cdot, t_n))$ and $p(\cdot, t_n)$, respectively.

$$\left\{ \begin{array}{l} \mathbf{U}_h^0 = \mathbf{U}_{0h} \\ \text{Given } (\mathbf{U}_h^n, p_h^n) \in \mathbf{X}_h \times M_h, \text{ find } (\mathbf{U}_h^{n+1}, p_h^{n+1}) \in \mathbf{X}_h \times M_h \text{ such that:} \\ \frac{1}{\Delta t} (\mathbf{U}_h^{n+1} - \mathbf{U}_h^n, \mathbf{V}_h) + b(\mathbf{u}_h^n; \mathbf{U}_h^{n+1}, \mathbf{V}_h) \\ + a(\mathbf{U}_h^{n+1}, \mathbf{V}_h) - (p_h^{n+1}, \nabla \cdot \mathbf{v}_h) + (\nabla \cdot \mathbf{u}_h^{n+1}, q_h) \\ + S_h(\mathbf{u}_h^n; (\mathbf{U}_h^{n+1}, p_h^{n+1}), (\mathbf{V}_h, q_h)) = \langle \bar{\mathbf{F}}^{n+1}, \mathbf{V}_h \rangle - c(\mathbf{U}_h^n, \mathbf{V}_h), \\ \forall (\mathbf{V}_h, q_h) \in \mathbf{X}_h \times M_h, \text{ for } n = 0, 1, \dots, N - 1. \end{array} \right. \tag{14}$$

Here, $\mathbf{U}_{0h} = (\mathbf{u}_{0h}, \theta_{0h})$ is the Stokes interpolate of \mathbf{U}_0 in \mathbf{X}_h (weakly free-divergence), and $\bar{\mathbf{F}}^{n+1} = (\bar{\mathbf{f}}^{n+1}, \bar{Q}^{n+1})$ with $\bar{\mathbf{f}}^{n+1}$ and \bar{Q}^{n+1} the average values of \mathbf{f} and Q , respectively, in $[t_n, t_{n+1}]$:

$$\bar{\mathbf{f}}^{n+1} = \frac{1}{\Delta t} \int_{t_n}^{t_{n+1}} \mathbf{f}(t) dt, \quad \bar{Q}^{n+1} = \frac{1}{\Delta t} \int_{t_n}^{t_{n+1}} Q(t) dt.$$

We propose also a alternative version of method (14), considering a discretization in time semi-implicit for the convection terms, while that of the remaining terms is fully implicit. That is:

$$\left\{ \begin{array}{l} \mathbf{U}_h^0 = \mathbf{U}_{0h} \\ \text{Given } (\mathbf{U}_h^n, p_h^n) \in \mathbf{X}_h \times M_h, \text{ find } (\mathbf{U}_h^{n+1}, p_h^{n+1}) \in \mathbf{X}_h \times M_h \text{ such that:} \\ \frac{1}{\Delta t} (\mathbf{U}_h^{n+1} - \mathbf{U}_h^n, \mathbf{V}_h) + A(\mathbf{u}_h^n; (\mathbf{U}_h^{n+1}, p_h^{n+1}), (\mathbf{V}_h, q_h)) \\ + S_h(\mathbf{u}_h^n; (\mathbf{U}_h^{n+1}, p_h^{n+1}), (\mathbf{V}_h, q_h)) = \langle \bar{\mathbf{F}}^{n+1}, \mathbf{V}_h \rangle, \\ \forall (\mathbf{V}_h, q_h) \in \mathbf{X}_h \times M_h, \text{ for } n = 0, 1, \dots, N - 1. \end{array} \right. \tag{15}$$

4 Analysis of the Discrete Models

In this section, we perform the numerical analysis of the proposed discrete models (14) and (15).

4.1 Technical Background

This section provides some technical results that are required for the numerical analysis.

Hypothesis 4.1 \mathbf{U}_{0h} is some interpolate of \mathbf{U}_0 in \mathbf{X}_h such that:

$$\|\mathbf{U}_{0h}\|_{\mathbf{L}^2} \leq C \|\mathbf{U}_0\|_{\mathbf{L}^2}, \tag{16}$$

for some positive constant C . Also:

$$\lim_{h \rightarrow 0} (\mathbf{U}_{0h}, \mathbf{V}) = (\mathbf{U}_0, \mathbf{V}), \quad \forall \mathbf{V} \in \mathbf{X}. \tag{17}$$

Hypothesis 4.2 The stabilization coefficients $\tau_{1,K}$, $\tau_{2,K}$, and $\tau_{3,K}$ satisfy the following conditions:

$$\alpha_1 h_K^2 < \tau_{1,K} \leq \alpha_2 h_K^2, \quad 0 < \tau_{2,K} \leq \beta h_K^2, \quad 0 < \tau_{3,K} \leq \gamma, \tag{18}$$

for all $K \in \mathcal{T}_h$, and some positive constants $\alpha_1, \alpha_2, \beta, \gamma$ independent of h .

This hypothesis is verified by the usual stabilization coefficients and, in particular, by those given by Chacón [18] or Codina [29] (these latter are used in numerical simulations). This assumption holds even in the convection-dominated regime.

Hypothesis 4.3 The operator Π_h is locally stable in L^2 -norm, i.e. there exists a positive constant C such that:

$$\|\Pi_h(\mathbf{v})\|_{L^2(K)} \leq C \|\mathbf{v}\|_{L^2(w_K)}, \quad \forall \mathbf{v} \in L^2(\Omega)^{d+2}, \tag{19}$$

where w_K is the union of all elements of \mathcal{T}_h that intersect K .

We also assume that:

$$\lim_{h \rightarrow 0} \|(I - \Pi_h)\boldsymbol{\varphi}\|_{L^2} = 0, \quad \forall \boldsymbol{\varphi} \in L^2(\Omega)^{d+2}. \tag{20}$$

This hypothesis is verified by the Scott–Zhang-like interpolation operator used in numerical tests (Cf. [19]). Note that, as a consequence of (18) and (19), there exist positive constants C_1, C_2, C_3 such that:

$$\|\Pi_{h,1}^*(\mathbf{v})\|_{\tau_1} \leq C_1 h \|\mathbf{v}\|_{L^2}, \quad \forall \mathbf{v} \in L^2(\Omega)^d. \tag{21}$$

$$\|\Pi_{h,2}^*(z)\|_{\tau_2} \leq C_2 h \|z\|_{L^2}, \quad \forall z \in L^2(\Omega). \tag{22}$$

$$\|\Pi_{h,3}^*(q)\|_{\tau_3} \leq C_3 \|q\|_{L^2}, \quad \forall q \in L^2(\Omega). \tag{23}$$

We also need the following discrete version of the Gronwall’s lemma:

Lemma 4.4 ([25], Lemma 10.4) *Let $\{\alpha_n\}_{n=0}^N, \{\beta_n\}_{n=0}^N$ be two finite sequences of non-negative real numbers such that:*

$$(1 - C_n \Delta t)\alpha_{n+1} \leq (1 + D_n \Delta t)\alpha_n + \beta_n, \quad \text{for } n = 0, 1, \dots, N - 1,$$

for two finite sequences of non-negative real numbers $\{C_n\}_{n=0}^N, \{D_n\}_{n=0}^N$. Assume that $\Delta t \leq 1/(2 \max\{C_0, \dots, C_{N-1}\})$. Then:

$$\max_{0 \leq n \leq N} \alpha_n \leq e^{2\Delta t S_N} \left(\alpha_0 + 2 \sum_{k=0}^{N-1} \beta_k \right), \tag{24}$$

where $S_N = \sum_{n=0}^{N-1} (C_n + D_n)$.

Also, we state a specific discrete inf–sup condition that enables to prove the stability of the pressure (Cf. [20], Theorem 2.3). To do that, we decompose $\overline{\Omega}$ into a finite union of macroelements:

$$\overline{\Omega} = \bigcup_{i=1}^R \mathcal{O}_i,$$

such that each \mathcal{O}_i is the support of the piecewise affine basis function associated to the node i . This decomposition is possible if no element of \mathcal{T}_h has all its nodes on Γ . Also, define the FE spaces:

$$\begin{aligned} V_h^l(\mathcal{O}_i) &= \{v_h \in C^0(\overline{\mathcal{O}_i}) \text{ such that } v_h|_K \in \mathbb{P}_1(K), \forall K \in \mathcal{T}_h \text{ such that } K \subset \mathcal{O}_i\}, \\ \mathcal{U}_h(\mathcal{O}_i) &= (V_h^l(\mathcal{O}_i) \cap H_0^1(\mathcal{O}_i))^d. \end{aligned}$$

Lemma 4.5 *Assume that Hypothesis 4.2 holds. Then, the following inf–sup condition is satisfied:*

$$\forall q_h \in M_h, \quad C \|q_h\|_{L^2} \leq \sup_{\mathbf{v}_h \in \mathcal{U}_h} \frac{(\nabla \cdot \mathbf{v}_h, q_h)}{\|\nabla(\mathbf{v}_h)\|_{\mathbf{L}^2}} + \|\Pi_{h,1}^*(\nabla q_h)\|_{\tau_1} + \left(\sum_{i=1}^R \left(\sup_{\mathbf{v}_h \in \mathcal{U}_h(\mathcal{O}_i)} \frac{(\nabla \cdot \mathbf{v}_h, q_h)_{\mathcal{O}_i}}{\|\nabla(\mathbf{v}_h)\|_{\mathbf{L}^2(\mathcal{O}_i)}} \right)^2 \right)^{1/2}, \tag{25}$$

for some positive constant C independent of h .

In the inf–sup condition (25), the first term in the right-hand bounds the large-scales components of ∇q_h that may be representable in \mathcal{U}_h , while the second one bounds the small-scales components that cannot be represented in \mathcal{U}_h . The third one gives some extra control on the high frequencies of ∇q_h possibly caused by the non-uniform regularity of the meshes.

When the family of triangulations is uniformly regular, that is there exists a positive constant α independent of h such that $\frac{h_K}{h} \geq \alpha, \forall K \in \mathcal{T}_h$, the above inf–sup condition (25) reduces to a simpler one (Cf. [20], Theorem 2.6):

$$\forall q_h \in M_h, \quad C \|q_h\|_{L^2} \leq \sup_{\mathbf{v}_h \in \mathcal{U}_h} \frac{(\nabla \cdot \mathbf{v}_h, q_h)}{\|\nabla(\mathbf{v}_h)\|_{\mathbf{L}^2}} + \|\Pi_{h,1}^*(\nabla q_h)\|_{\tau_1}. \tag{26}$$

Our analysis is based upon a compactness result on Nikolskii spaces stated in Simon [51]. Let B a Banach space. The Nikolskii space of order $\sigma \in [0, 1]$ and exponent $p \in [0, +\infty]$ associated with B and a time interval $(0, T)$ is defined as:

$$N^{\sigma,p}(0, T; B) = \left\{ f \in L^p(0, T; B) \text{ such that } \|f\|_{\hat{N}^{\sigma,p}} < +\infty \right\},$$

with:

$$\|f\|_{\hat{N}^{\sigma,p}} = \sup_{\delta > 0} \frac{1}{\delta^\sigma} \|\Delta_\delta f\|_{L^p(0, T-\delta; B)},$$

where $\Delta_\delta f = f(t + \delta) - f(t), 0 \leq t \leq T - \delta$. The space $N^{\sigma,p}(0, T; B)$ endowed with the norm:

$$\|f\|_{L^p(0, T; B)} + \|f\|_{\hat{N}^{\sigma,p}},$$

is a Banach space. Simon’s theorem is stated as follows.

Lemma 4.6 *Let E, F and G be Banach spaces such that $E \hookrightarrow F \hookrightarrow G$, where the injection $E \hookrightarrow F$ is compact. Then, the injection:*

$$L^p(0, T; E) \cap N^{\sigma,p}(0, T; G) \hookrightarrow L^p(0, T; F), \quad \text{with } 0 < \sigma < 1 \text{ and } 1 \leq p \leq +\infty,$$

holds and it is compact.

4.2 Stability Analysis

We define the following discrete functions:

- $U_h = (\mathbf{u}_h, \theta_h) : [0, T] \rightarrow X_h$ is the piecewise linear in time function such that $U_h(t_n) = U_h^n$.

- $\mathbf{m}_h : [0, T] \rightarrow V_h^{l-1}, c_h : [0, T] \rightarrow V_h^{m-1}$ and $d_h : [0, T] \rightarrow V_h^{n-1}$ are the piecewise linear in time functions such that:

$$\begin{aligned} \mathbf{m}_h(t^{n+1}) &= \mathbf{m}_h^{n+1} := \Pi_{h,1}^* \left(\mathbf{u}_h^n \cdot \nabla \mathbf{u}_h^{n+1} + \nabla p_h^{n+1} \right), \\ c_h(t^{n+1}) &= c_h^{n+1} := \Pi_{h,2}^* \left(\mathbf{u}_h^n \cdot \nabla \theta_h^{n+1} \right), \\ d_h(t^{n+1}) &= d_h^{n+1} := \Pi_{h,3}^* \left(\nabla \cdot \mathbf{u}_h^{n+1} \right). \end{aligned}$$

- $\tilde{p}_h : [0, T] \rightarrow M_h$ is the piecewise constant in time function that takes the value p_h^{n+1} on (t_n, t_{n+1}) .
- $P_h : [0, T] \rightarrow M_h$ is the primitive of \tilde{p}_h :

$$P_h(t) = \int_0^t \tilde{p}_h(s) ds.$$

Theorem 4.7 Under hypotheses (16), (18) and (19) there exists a positive constant C such that if $h\sqrt{\Delta t} \leq \frac{C}{\lambda}$, then the discrete problem (14) admits a unique solution that satisfies the following estimates:

$$\begin{aligned} &\|U_h\|_{L^\infty(\mathbf{L}^2)} + \sqrt{\underline{\mu}} \|U_h\|_{L^2(X)} \\ &\quad + \|\mathbf{m}_h\|_{L^2(\mathbf{L}_{\tau_1}^2)} + \|c_h\|_{L^2(\mathbf{L}_{\tau_2}^2)} + \|d_h\|_{L^2(\mathbf{L}^2)} \leq C_1 \left(1 + (\sqrt{\lambda} + h\lambda)\sqrt{T} \right) D_{\lambda,\mu} \end{aligned} \tag{27}$$

$$\|U_h\|_{N^{1/4,2}(\mathbf{L}^2)} \leq C_2 D_{\lambda,\mu} \tag{28}$$

$$\|P_h\|_{L^\infty(\mathbf{L}^2)} \leq C_2 D_{\lambda,\mu} \tag{29}$$

where $\underline{\mu} = \min\{r, s\}$, C_1 is a positive constant independent of r, s, λ, h and Δt , $D_{\lambda,\mu}$ is the constant given by $D_{\lambda,\mu} := e^{\lambda T} \left(\|U_0\|_{\mathbf{L}^2} + \underline{\mu}^{-1/2} \|F\|_{L^2(X)} \right)$ and C_2 is a positive constant independent of h and Δt .

Proof We proceed by steps. Throughout the proof, we shall denote by C constants that may vary from a line to another, but which are always independent of h and Δt .

Step 1: Existence and uniqueness of solution Problem (14) is equivalent to N square linear systems of dimension $\dim(X_h) + \dim(M_h)$. Then, the existence of solution is equivalent to the uniqueness. To prove the uniqueness, we shall assume that a solution exists and prove the estimates (27)–(29) of this solution in terms of the data. Then, the difference of two solutions satisfies the homogenous problem and necessarily this difference should vanish under these estimates.

Step 2: Velocity and temperature estimates We set $V_h = U_h^{n+1}$ and $q_h = p_h^{n+1}$ in (14). Observe that:

$$2 \left(U_h^{n+1} - U_h^n, U_h^{n+1} \right) = \|U_h^{n+1}\|_{\mathbf{L}^2}^2 - \|U_h^n\|_{\mathbf{L}^2}^2 + \|\mathbf{u}_h^{n+1} - \mathbf{u}_h^n\|_{\mathbf{L}^2}^2 + \|\theta_h^{n+1} - \theta_h^n\|_{L^2}^2,$$

and:

$$a \left(U_h^{n+1}, U_h^{n+1} \right) \geq \underline{\mu} \|U_h^{n+1}\|_X^2.$$

Thus, we obtain:

$$\begin{aligned} &\frac{1}{2\Delta t} \left(\|U_h^{n+1}\|_{\mathbf{L}^2}^2 - \|U_h^n\|_{\mathbf{L}^2}^2 \right) + \underline{\mu} \|U_h^{n+1}\|_X^2 + \|\mathbf{m}_h^{n+1}\|_{\tau_1}^2 + \|c_h^{n+1}\|_{\tau_2}^2 + \|d_h^{n+1}\|_{\tau_3}^2 \\ &\leq \left\langle \tilde{F}^{n+1}, U_h^{n+1} \right\rangle + \lambda \left(\theta_h^n, \mathbf{u}_{hd}^n \right) - S_h^{buo} \left(\mathbf{u}_h^n, \left(U_h^{n+1}, p_h^{n+1} \right), \left(U_h^{n+1}, p_h^{n+1} \right) \right), \end{aligned} \tag{30}$$

Applying the Cauchy–Schwartz inequality:

$$\left\langle \bar{F}^{n+1}, U_h^{n+1} \right\rangle \leq \frac{1}{2} \underline{\mu}^{-1} \left\| \bar{F}^{n+1} \right\|_{X'}^2 + \frac{1}{2} \underline{\mu} \left\| U_h^{n+1} \right\|_X^2. \tag{31}$$

Also:

$$\lambda \left(\theta_h^n, u_{hd}^n \right) \leq \lambda \left\| U_h^n \right\|_{L^2}^2. \tag{32}$$

Moreover, as:

$$\lambda \left(\Pi_{h,1}^* \left(u_h^n \cdot \nabla u_{hd}^{n+1} + \partial_d p_h^{n+1} \right), \Pi_{h,1}^* \left(\theta_h^{n+1} \right) \right)_{\tau_1} \leq \frac{1}{2} \left\| m_h^{n+1} \right\|_{\tau_1}^2 + \frac{\lambda^2}{2} \left\| \Pi_{h,1}^* \left(\theta_h^{n+1} \right) \right\|_{\tau_1}^2,$$

and:

$$\lambda \left(\Pi_{h,2}^* (u_{hd}^{n+1}), \Pi_{h,2}^* \left(u_h^n \cdot \nabla \theta_h^{n+1} \right) \right)_{\tau_2} \leq \frac{1}{2} \left\| c_h^{n+1} \right\|_{\tau_2}^2 + \frac{\lambda^2}{2} \left\| \Pi_{h,2}^* \left(u_{hd}^{n+1} \right) \right\|_{\tau_2}^2,$$

then, taking in account (21) and (22),

$$S_h^{buo} \left(u_h^n; \left(U_h^{n+1}, p_h \right), \left(U_h^{n+1}, p_h \right) \right) \leq \frac{1}{2} \left\| m_h^{n+1} \right\|_{\tau_1}^2 + \frac{1}{2} \left\| c_h^{n+1} \right\|_{\tau_2}^2 + C \lambda^2 h^2 \left\| U_h^{n+1} \right\|_{L^2}^2. \tag{33}$$

Thus, from (30) and estimates (31)–(33), we obtain:

$$\begin{aligned} & \frac{1}{\Delta t} \left(\left\| U_h^{n+1} \right\|_{L^2}^2 - \left\| U_h^n \right\|_{L^2}^2 \right) + \underline{\mu} \left\| U_h^{n+1} \right\|_X^2 + \left\| m_h^{n+1} \right\|_{\tau_1}^2 + \left\| c_h^{n+1} \right\|_{\tau_2}^2 + 2 \left\| d_h^{n+1} \right\|_{\tau_3}^2 \\ & \leq \underline{\mu}^{-1} \left\| \bar{F}^{n+1} \right\|_{X'}^2 + \lambda \left\| U_h^n \right\|_{L^2}^2 + \hat{\lambda} \left\| U_h^{n+1} \right\|_{L^2}^2, \quad \text{for } n = 0, 1, \dots, N-1, \end{aligned} \tag{34}$$

with $\hat{\lambda} = C \lambda^2 h^2$.

Now, we apply the discrete Gronwall’s Lemma 4.4 with:

$$\alpha_n = \left\| U_h^n \right\|_{L^2}^2, \quad \beta_n = \Delta t \underline{\mu}^{-1} \left\| \bar{F}^{n+1} \right\|_{X'}^2, \quad C_n = \hat{\lambda} \quad \text{and} \quad D_n = \lambda.$$

If $h \sqrt{\Delta t} \leq \frac{1}{\sqrt{2C} \lambda}$ then $\Delta t \leq \frac{1}{2\hat{\lambda}}$, we deduce:

$$\max_{0 \leq n \leq N} \left\| U_h^n \right\|_{L^2} \leq C D_{\lambda, \mu}, \tag{35}$$

due to (16) and $\sum_{k=0}^{N-1} \Delta t \left\| F^{k+1} \right\|_{X'}^2 \leq \left\| F \right\|_{L^2(X')}^2$.

Summing with respect to n in (34), we obtain:

$$\begin{aligned} & \left\| U_h^N \right\|_{L^2}^2 + \Delta t \left(\underline{\mu} \sum_{k=0}^{N-1} \left\| U_h^{k+1} \right\|_X^2 + \sum_{k=0}^{N-1} \left\| m_h^{k+1} \right\|_{\tau_1}^2 + \sum_{k=0}^{N-1} \left\| c_h^{k+1} \right\|_{\tau_2}^2 + 2 \sum_{k=0}^{N-1} \left\| d_h^{k+1} \right\|_{\tau_3}^2 \right) \\ & \leq \left\| U_h^0 \right\|_{L^2}^2 + \underline{\mu}^{-1} \sum_{k=0}^{N-1} \Delta t \left\| F^{k+1} \right\|_{X'}^2 + \lambda \Delta t \sum_{k=0}^{N-1} \left\| U_h^k \right\|_{L^2}^2 + \hat{\lambda} \Delta t \sum_{k=0}^{N-1} \left\| U_h^{k+1} \right\|_{L^2}^2 \\ & \leq C \left(e^{-\lambda T} + \lambda T + \hat{\lambda} T \right) D_{\lambda, \mu}^2 \leq C \left(1 + \lambda T + \lambda^2 h^2 T \right) D_{\lambda, \mu}^2, \end{aligned} \tag{36}$$

taking into account (35). Note that:

$$\|U_h\|_{L^\infty(L^2)} = \max_{0 \leq n \leq N} \|U_h^n\|_{L^2}, \quad \|U_h\|_{L^2(X)}^2 \leq \sum_{k=0}^{N-1} \Delta t \|U_h^{k+1}\|_X^2,$$

and also:

$$\begin{aligned} \|m_h\|_{L^2(L^2_{\tau_1})}^2 &\leq C \sum_{k=0}^{N-1} \Delta t \|m_h^{k+1}\|_{\tau_1}^2, \quad \|c_h\|_{L^2(L^2_{\tau_2})}^2 \leq C \sum_{k=0}^{N-1} \Delta t \|c_h^{k+1}\|_{\tau_2}^2, \\ \|d_h\|_{L^2(L^2)}^2 &\leq C \sum_{k=0}^{N-1} \Delta t \|d_h^{k+1}\|_{\tau_3}^2. \end{aligned}$$

So, (27) follows from (35) and (36).

Step 3: Time primitive of the pressure estimate We define the following discrete functions:

- $\tilde{U}_h = (\tilde{u}_h, \tilde{\theta}_h) : [0, T] \rightarrow X_h$ is the piecewise constant in time function that takes the value $U_h^{n+1} = (u_h^{n+1}, \theta_h^{n+1})$ on (t_n, t_{n+1}) .
- $\tilde{U}_h^- = (\tilde{u}_h^-, \tilde{\theta}_h^-) : [0, T] \rightarrow X_h$ is the piecewise constant in time function that takes the value $U_h^n = (u_h^n, \theta_h^n)$ on (t_n, t_{n+1}) .
- $\tilde{m}_h : [0, T] \rightarrow V_h^{m-1}$, $\tilde{c}_h : [0, T] \rightarrow V_h^{n-1}$ and $\tilde{d}_h : [0, T] \rightarrow V_h^{n-1}$ are the piecewise constant in time functions that take the values m_h^{n+1} , c_h^{n+1} and d_h^{n+1} , respectively, on (t_n, t_{n+1}) .
- $\tilde{F}_h : [0, T] \rightarrow X'$ is the piecewise constant in time function with values on X' that takes the value F_h^{n+1} in (t_n, t_{n+1}) .

With this notation, method (14) can be written as:

$$\begin{cases} (\partial_t U_h(t), V_h) + b(\tilde{u}_h^-(t); \tilde{U}_h(t), V_h) \\ + a(\tilde{U}_h(t), V_h) + c(\tilde{U}_h^-(t), V_h) - (\tilde{p}_h(t), \nabla \cdot v_h) + (\nabla \cdot \tilde{u}_h(t), q_h) \\ + S_h(\tilde{u}_h^-(t); (\tilde{U}_h(t), \tilde{p}_h(t)), (V_h, q_h)) = \langle \tilde{F}_h(t), V_h \rangle, \\ \text{a.e. in } [0, T], \forall (V_h, q_h) \in X_h \times M_h. \end{cases} \tag{37}$$

For brevity, we have reduced the proof to the simpler case of uniformly regular meshes and used the inf-sup condition (26) for $P_h(t) \in M_h$. Setting $V_h = \tilde{V}_h := (v_h, 0) \in X_h$ and $q_h = 0$ in (37), and integrating in $(0, t)$, for $t \in [0, T]$, we have:

$$(P_h(t), \nabla \cdot v_h) = (U_h(t) - U_{0h}, \tilde{V}_h) - \int_0^t \langle \mathcal{F}_h(s), \tilde{V}_h \rangle ds, \tag{38}$$

where $\mathcal{F}_h(s) \in X'_h$ is defined a.e. in $(0, T)$ by:

$$\langle \mathcal{F}_h(s), \tilde{V}_h \rangle = \langle \mathcal{A}_h(s), \tilde{V}_h \rangle - S_h(\tilde{u}_h^-(s); (\tilde{U}_h(s), \tilde{p}_h(s)), (\tilde{V}_h, 0)), \quad \forall \tilde{V}_h \in X_h,$$

with $\mathcal{A}_h(s) \in X'$ such that:

$$\langle \mathcal{A}_h(s), V \rangle = \langle \tilde{F}_h(s), V \rangle - b(\tilde{u}_h^-(s); \tilde{U}_h(s), V) - a(\tilde{U}_h(s), V) - c(\tilde{U}_h^-(s), V),$$

for any $V \in X$. Thanks to the continuity of the forms b , a and c :

$$\|\mathcal{A}_h(s)\|_{X'} \leq C \left(\|\tilde{F}_h(s)\|_{X'} + \left(\|\tilde{u}_h^-(s)\|_{H^1_0} + \bar{\mu} \right) \|\tilde{U}_h(s)\|_X + \lambda \|\tilde{\theta}_h^-(s)\|_{L^2} \right), \tag{39}$$

where $\bar{\mu} = \max\{r, s\}$.

Now, we are going to estimate each of the terms in $S_h(\tilde{\mathbf{u}}_h^-(s); (\tilde{\mathbf{U}}_h(s), \tilde{p}_h(s)), (\tilde{\mathbf{V}}_h, 0))$. Firstly, observe that:

$$\|\Pi_{h,1}^*(\tilde{\mathbf{u}}_h^-(s) \cdot \nabla \mathbf{v}_h)\|_{\tau_1} \leq C \sqrt{h} \|\tilde{\mathbf{u}}_h^-(s)\|_{\mathbf{H}_0^1} \|\nabla \mathbf{v}_h\|_{\mathbf{L}^2}. \tag{40}$$

In fact,

$$\begin{aligned} \|\Pi_{h,1}^*(\tilde{\mathbf{u}}_h^-(s) \cdot \nabla \mathbf{v}_h)\|_{\tau_1}^2 &\leq C \sum_{K \in \mathcal{T}_h} h_K^2 \|\tilde{\mathbf{u}}_h^-(s) \cdot \nabla \mathbf{v}_h\|_{\mathbf{L}^2(w_K)}^2 \\ &\leq C \sum_{K \in \mathcal{T}_h} h_K^2 \|\tilde{\mathbf{u}}_h^-(s)\|_{\mathbf{L}^6(w_K)}^2 \|\nabla \mathbf{v}_h\|_{\mathbf{L}^3(w_K)}^2 \leq C \|\tilde{\mathbf{u}}_h^-(s)\|_{\mathbf{H}_0^1}^2 \sum_{K \in \mathcal{T}_h} h_K^{2-\frac{d}{3}} \|\nabla \mathbf{v}_h\|_{\mathbf{L}^2(w_K)}^2 \\ &\leq C \|\tilde{\mathbf{u}}_h^-(s)\|_{\mathbf{H}_0^1}^2 h \|\nabla \mathbf{v}_h\|_{\mathbf{L}^2}^2, \end{aligned}$$

where we have used (18), (19), the Young’s inequality, the Sobolev embeddings and the local inverse inequality between $W^{1,3}(K)$ and $H^1(K)$ (Cf. [12], Proposition 5.1).

Then, using (40):

$$S_h^{mom} \leq \|\tilde{\mathbf{m}}_h(s)\|_{\tau_1} \|\Pi_{h,1}^*(\tilde{\mathbf{u}}_h^-(s) \cdot \nabla \mathbf{v}_h)\|_{\tau_1} \leq C \sqrt{h} \|\tilde{\mathbf{m}}_h(s)\|_{\tau_1} \|\tilde{\mathbf{u}}_h^-(s)\|_{\mathbf{H}_0^1} \|\nabla \mathbf{v}_h\|_{\mathbf{L}^2}. \tag{41}$$

Also:

$$S_h^{div} \leq \|\tilde{\mathbf{d}}_h(s)\|_{\tau_3} \|\Pi_{h,3}^*(\nabla \cdot \mathbf{v}_h)\|_{\tau_3} \leq C \|\tilde{\mathbf{d}}_h(s)\|_{\tau_3} \|\nabla \mathbf{v}_h\|_{\mathbf{L}^2}, \tag{42}$$

using (23). Furthermore:

$$\begin{aligned} (\Pi_{h,1}^*(\tilde{\mathbf{u}}_h^-(s) \cdot \nabla v_{hd}), \Pi_{h,1}^*(\tilde{\theta}_h(s)))_{\tau_1} &\leq \|\Pi_{h,1}^*(\tilde{\mathbf{u}}_h^-(s) \cdot \nabla \mathbf{v}_h)\|_{\tau_1} \|\Pi_{h,1}^*(\tilde{\theta}_h(s))\|_{\tau_1} \\ &\leq C h^{3/2} \|\tilde{\theta}_h(s)\|_{L^2} \|\tilde{\mathbf{u}}_h^-(s)\|_{\mathbf{H}_0^1} \|\nabla \mathbf{v}_h\|_{\mathbf{L}^2}, \end{aligned} \tag{43}$$

and:

$$\begin{aligned} (\Pi_{h,2}^*(v_{hd}), \Pi_{h,2}^*(\tilde{\mathbf{u}}_h^-(s) \cdot \nabla \tilde{\theta}_h(s)))_{\tau_2} &\leq \|\Pi_{h,2}^*(v_{hd})\|_{\tau_2} \|\tilde{\mathbf{c}}_h(s)\|_{\tau_2} \\ &\leq C h \|\tilde{\mathbf{c}}_h(s)\|_{\tau_2} \|\nabla \mathbf{v}_h\|_{\mathbf{L}^2}, \end{aligned} \tag{44}$$

using (22) and Korn’s inequality. Thus, the estimate (39) and the estimates (41)–(44) yield:

$$\begin{aligned} \|\mathcal{F}_h(s)\|_{X'_h} &\leq C \left(\|\tilde{\mathbf{F}}_h(s)\|_{X'_h} + (\|\tilde{\mathbf{u}}_h^-(s)\|_{\mathbf{H}_0^1} + \bar{\mu}) \|\tilde{\mathbf{U}}_h(s)\|_X + \lambda \|\tilde{\theta}_h^-(s)\|_{L^2} \right. \\ &\quad \left. + (\|\tilde{\mathbf{m}}_h(s)\|_{\tau_1} + \lambda \|\tilde{\theta}_h(s)\|_{L^2}) \|\tilde{\mathbf{u}}_h^-(s)\|_{\mathbf{H}_0^1} + \lambda \|\tilde{\mathbf{c}}_h(s)\|_{\tau_2} + \|\tilde{\mathbf{d}}_h(s)\|_{\tau_3} \right). \end{aligned}$$

Due to estimate (27), this implies that $\mathcal{F}_h \in L^1(X'_h)$ and:

$$\|\mathcal{F}_h\|_{L^1(X'_h)} \leq C. \tag{45}$$

From (38):

$$\begin{aligned} (P_h(t), \nabla \cdot \mathbf{v}_h) &\leq C \left(\|\mathbf{U}_h\|_{L^\infty(\mathbf{L}^2)} + \|\mathbf{U}_{0h}\|_{\mathbf{L}^2} + \|\mathcal{F}_h\|_{L^1(X'_h)} \right) \|\nabla \mathbf{v}_h\|_{\mathbf{L}^2} \\ &\leq C \|\nabla \mathbf{v}_h\|_{\mathbf{L}^2}, \end{aligned} \tag{46}$$

where we have used that $\|\tilde{\mathbf{V}}_h\|_X = \|\nabla \mathbf{v}_h\|_{\mathbf{L}^2}$, and estimates (27) and (45).

Moreover, as $\Pi_{h,1}$ is linear:

$$\Pi_{h,1}^*(\nabla P_h(t)) = \int_0^t \Pi_{h,1}^*(\nabla \tilde{p}_h(s)) ds = \int_0^t \tilde{\mathbf{m}}_h(s) ds - \int_0^t \Pi_{h,1}^*(\tilde{\mathbf{u}}_h^-(s) \cdot \nabla \tilde{\mathbf{u}}_h(s)) ds.$$

Then:

$$\begin{aligned} \left\| \Pi_{h,1}^*(\nabla P_h(t)) \right\|_{\tau_1} &\leq \int_0^t \|\tilde{\mathbf{m}}_h(s)\|_{\tau_1} ds + \int_0^t \left\| \Pi_{h,1}^*(\tilde{\mathbf{u}}_h^-(s) \cdot \nabla \tilde{\mathbf{u}}_h(s)) \right\|_{\tau_1} ds \\ &\leq C \left(\|\tilde{\mathbf{m}}_h\|_{L^1(\mathbf{L}^2_{\tau_1})} + \|\tilde{\mathbf{u}}_h^-\|_{L^2(\mathbf{H}^1)}^2 + \|\tilde{\mathbf{u}}_h\|_{L^2(\mathbf{H}^1)}^2 \right), \end{aligned}$$

using (40) and Young’s inequality. Now, taking into account again (27), we deduce that:

$$\left\| \Pi_{h,1}^*(\nabla P_h(t)) \right\|_{\tau_1} \leq C. \tag{47}$$

From (26) and estimates (46) and (47), the pressure estimate (29) follows.

Step 4: Velocity and temperature time increment estimates Setting $q_h = \tilde{p}_h(t)$ in (37) and integrating in $(t, t + \delta)$ for $t \in [0, T - \delta]$ yields:

$$(\Delta_\delta \mathbf{U}_h(t), \mathbf{V}_h) = \int_t^{t+\delta} \langle \mathcal{G}_h(s), \mathbf{V}_h \rangle, ds, \quad \forall \mathbf{V}_h \in \mathbf{X}_h, \tag{48}$$

where $\Delta_\delta \mathbf{U}_h(t) = \mathbf{U}_h(t + \delta) - \mathbf{U}_h(t)$ and $\mathcal{G}_h(s) \in \mathbf{X}'_h$ is defined a.e. in $(0, T)$ by:

$$\langle \mathcal{G}_h(s), \mathbf{V}_h \rangle = \langle \mathcal{A}_h(s), \mathbf{V}_h \rangle - S_h(\tilde{\mathbf{u}}_h^-(s); (\tilde{\mathbf{U}}_h(s), \tilde{p}_h(s)), (\mathbf{V}_h, \tilde{p}_h(s))), \quad \forall \mathbf{V}_h \in \mathbf{X}_h.$$

We have to estimate each of the terms in $S_h(\tilde{\mathbf{u}}_h^-(s); (\tilde{\mathbf{U}}_h(s), \tilde{p}_h(s)), (\mathbf{V}_h, \tilde{p}_h(s)))$. To do it, observe that:

$$\left\| \Pi_{h,1}^*(\tilde{\mathbf{u}}_h^-(s) \cdot \nabla \mathbf{v}_h + \nabla \tilde{p}_h(s)) \right\|_{\tau_1} \leq \|\tilde{\mathbf{m}}_h(s)\|_{\tau_1} + \left\| \Pi_{h,1}^*(\tilde{\mathbf{u}}_h^-(s) \cdot \nabla (\mathbf{v}_h - \tilde{\mathbf{u}}_h(s))) \right\|_{\tau_1}$$

The last term can be bounded as in (40), so using again (27):

$$\left\| \Pi_{h,1}^*(\tilde{\mathbf{u}}_h^-(s) \cdot \nabla \mathbf{v}_h + \nabla \tilde{p}_h(s)) \right\|_{\tau_1} \leq C \|\mathbf{V}_h\|_{\mathbf{X}}. \tag{49}$$

Then, following a similar argument to that in Step 2, we obtain: $\mathcal{G}_h \in L^1(\mathbf{X}'_h)$ and:

$$\|\mathcal{G}_h\|_{L^1(\mathbf{X}'_h)} \leq C. \tag{50}$$

Now, taking $\mathbf{V}_h = \Delta_\delta \mathbf{U}_h(t)$ in (48) and integrating in $(0, T - \delta)$ we have:

$$\begin{aligned} \int_0^{T-\delta} \|\Delta_\delta \mathbf{U}_h(t)\|_{\mathbf{L}^2}^2 dt &= \int_0^{T-\delta} \int_t^{t+\delta} \langle \mathcal{G}_h(s), \Delta_\delta \mathbf{U}_h(t) \rangle ds dt \\ &= \int_0^T \int_{s-\delta}^s \langle \mathcal{G}_h(s), \widehat{\Delta_\delta \mathbf{U}_h}(t) \rangle dt ds, \end{aligned}$$

where in the last equality we have applied Fubini’s theorem, denoting by \widehat{v} the extension by zero of a function v outside $[0, T - \delta]$. Then:

$$\begin{aligned} \int_0^{T-\delta} \|\Delta_\delta \mathbf{U}_h(t)\|_{\mathbf{L}^2}^2 dt &\leq \int_0^T \left(\|\mathcal{G}_h(s)\|_{\mathbf{X}'_h} \int_{s-\delta}^s \|\Delta_\delta \mathbf{U}_h(t)\|_{\mathbf{X}} dt \right) ds \\ &\leq \int_0^T \left(\|\mathcal{G}_h(s)\|_{\mathbf{X}'_h} \delta^{1/2} \left(\int_{s-\delta}^s \|\Delta_\delta \mathbf{U}_h(t)\|_{\mathbf{X}}^2 dt \right)^{1/2} \right) ds \\ &\leq \delta^{1/2} \|\mathcal{G}_h\|_{L^1(\mathbf{X}'_h)} \|\Delta_\delta \mathbf{U}_h\|_{\mathbf{L}^2(\mathbf{X})} \leq \delta^{1/2} \|\mathcal{G}_h\|_{L^1(\mathbf{X}'_h)} \|\mathbf{U}_h\|_{\mathbf{L}^2(\mathbf{X})} \leq C \delta^{1/2}, \end{aligned}$$

taking into account estimates (50) and (27). Consequently, estimate (28) follows. □

For the discrete problem (15) we obtain a result similar to the previous one, but we need to assume a restriction on the time step.

Theorem 4.8 Assume that (16), (18), (19) hold and also that $\Delta t \leq \frac{1}{4\hat{\lambda}}$. Then, there exists a positive constant C such that if $h \leq \frac{C}{\sqrt{\hat{\lambda}}}$, the discrete problem (15) admits a unique solution that satisfies the estimates (27)–(29).

Proof We proceed as in proof of Theorem 4.7 to obtain estimate (34), but now with $\hat{\lambda} = \lambda(1 + C\lambda h^2)$. If $h \leq \frac{1}{\sqrt{C\lambda}}$, then $\Delta t \leq \frac{1}{2\hat{\lambda}}$ and we can apply the discrete Gronwall’s lemma 4.4 with:

$$\alpha_n = \|U_h^n\|_{L^2}^2, \quad \beta_n = \Delta t \mu^{-1} \|\bar{F}^{n+1}\|_{X'}^2, \quad C_n = \hat{\lambda} \quad \text{and} \quad D_n = 0.$$

From here, we again deduce (35) and the rest of the proof remains the same. □

Remark 4.9 The stability requirements for the discretization parameters are due to the interaction between temperature and velocity, in both macro and micro scales, that is produced by buoyancy effects. The implicit discretization of the macro-scales buoyancy term in method (15) allows independent restrictions for the mesh size and the time step (Theorem 4.8). However a fully implicit discretization would not improve these restrictions because an implicit discretization of convective terms also leads to the estimate (34).

4.3 Convergence Analysis

The convergence of methods (14) and (15) reads as follows.

Theorem 4.10 Assume that Hypotheses 4.1–4.3 hold. Then, the sequence $\{U_h, P_h\}_{h>0}$ contains a sub-sequence $\{U_{h'}, P_{h'}\}_{h'>0}$ that is weakly convergent in $L^2(0, T; X) \times L^2(0, T; L^2(\Omega))$ to a weak solution (U, P) of problem (2). Moreover, $\{U_{h'}\}_{h'>0}$ strongly converges to U in $L^2(0, T; H^s(\Omega)^{d+1})$, for $0 \leq s < 1$, and weakly- $*$ converges in $L^\infty(0, T; L^2(\Omega)^{d+1})$, and $\{P_{h'}\}_{h'>0}$ weakly- $*$ converges to P in $L^\infty(0, T; L^2(\Omega))$.

Proof We proceed by steps.

Step 1: Extraction of convergent subsequences From the estimates (27) and (28), the sequence $\{U_h\}_{h>0}$ is uniformly bounded in $L^\infty(0, T; L^2(\Omega)^{d+1})$, in $L^2(0, T; X)$ and in $N^{1/4,2}(0, T; L^2(\Omega)^{d+1})$. Application of Lemma 4.6 with $E = X$, $F = H^s(\Omega)^{d+1}$, for $0 \leq s < 1$, and $G = L^2(\Omega)^{d+1}$ ensures its compactness in $L^2(0, T; H^s(\Omega)^{d+1})$, for $0 \leq s < 1$. Then, the sequence $\{U_h = (u_h, \theta_h)\}_{h>0}$ contains a sub-sequence (that we denote in the same way) strongly convergent in $L^2(0, T; H^s(\Omega)^{d+1})$, for $0 \leq s < 1$, weakly in $L^2(0, T; X)$ and weakly- $*$ in $L^\infty(0, T; L^2(\Omega)^{d+1})$ to some $U = (u, \theta)$. Moreover, P_h is uniformly bounded in $L^\infty(0, T; L^2(\Omega))$, so $\{P_h\}_{h>0}$ contains a sub-sequence (that we denote in the same way) weakly- $*$ convergent in this space to some P . We give in the sequel a sketch of the proof showing that (U, P) is a weak solution of (2), with P a time primitive of the physical pressure p , namely $p = \partial_t P$.

Also, note that by (27) the sequence $\{\tilde{U}_h\}_{h>0}$ is uniformly bounded in $L^\infty(0, T; L^2(\Omega)^{d+1})$ and $L^2(0, T; X)$. Then, it contains a sub-sequence (that we denote in the same way) weakly convergent in $L^2(0, T; X)$ and weakly- $*$ convergent in $L^\infty(0, T; L^2(\Omega)^{d+1})$ to some \tilde{U} . In fact, $\tilde{U} = U$ since it can be proved that $\{\tilde{U}_h\}_{h>0}$ also strongly converges in $L^2(0, T; L^2(\Omega)^{d+1})$ to U (Cf. [25], Theorem 10.2). Similarly, $\{\tilde{U}_h^-\}_{h>0}$ strongly converges in $L^2(0, T; L^2(\Omega)^{d+1})$ to U .

Step 2: Pass to the limit We reformulate problem (37) as:

$$\left\{ \begin{aligned} & - \int_0^T (\mathbf{U}_h(t), \mathbf{V}_h) \varphi'(t) dt - \langle \mathbf{U}_{h0}, \mathbf{V}_h \rangle \varphi(0) + \int_0^T b(\tilde{\mathbf{u}}_h^-(t); \tilde{\mathbf{U}}_h(t), \mathbf{V}_h) \varphi(t) dt \\ & + \int_0^T a(\tilde{\mathbf{U}}_h(t), \mathbf{V}_h) \varphi(t) dt + \int_0^T c(\tilde{\mathbf{U}}_h^-(t), \mathbf{V}_h) \varphi(t) dt \\ & + \int_0^T (P_h(t), \nabla \cdot \mathbf{v}_h) \varphi'(t) dt + \int_0^T (\nabla \cdot \tilde{\mathbf{u}}_h, q_h) \varphi(t) dt \\ & + \int_0^T S_h(\tilde{\mathbf{u}}_h^-(t); (\tilde{\mathbf{U}}_h(t), \tilde{p}_h(t)), (\mathbf{V}_h, q_h)) \varphi(t) dt = \int_0^T \langle \tilde{\mathbf{F}}_h(t), \mathbf{V}_h \rangle \varphi(t) dt, \\ & \forall \mathbf{V}_h \in \mathbf{X}_h, \forall q_h \in M_h, \forall \varphi \in \mathcal{D}([0, T]) \text{ such that } \varphi(T) = 0. \end{aligned} \right. \tag{51}$$

We consider the space

$$\mathcal{D}(\overline{\Omega}, \Gamma_D) = \{ \varphi \in \mathcal{D}(\overline{\Omega}) \text{ such that } \varphi = 0 \text{ in a neighborhood of } \Gamma_D \}$$

which is dense in $H_D^1(\Omega)$ (Cf. [11]) Let $\mathbf{V} = (\mathbf{v}, z)$ be a function in $\mathbf{X} \cap [\mathcal{D}(\Omega)^d \times \mathcal{D}(\overline{\Omega}, \Gamma_D)]$ and consider $\mathbf{V}_h = (\mathbf{v}_h, z_h)$ some interpolate of \mathbf{V} in \mathbf{X}_h that strongly converges to \mathbf{V} in \mathbf{X} . Also, we consider a function $q \in M \cap \mathcal{D}(\Omega)$ and some interpolate $q_h \in M_h$ that strongly converges to q in M . The stability results previously obtained allow to pass to the limit in the Galerkin terms by rather standard arguments (see [25], Sect 10.4). Also, the stabilization terms S_h^{mom} and S_h^{div} vanish in the limit following the convergence analysis performed in [21, 22]. Thus, here we just detail the pass to the limit in the terms involving temperature. *Buoyancy term* As $\{\tilde{\theta}_h^-\}_{h>0}$ strongly converges to θ in $L^2(0, T; L^2(\Omega))$:

$$\lim_{(h, \Delta t) \rightarrow 0} \int_0^T (\tilde{\theta}_h^-(t), v_{hd}) \varphi(t) dt = \int_0^T (\theta(t), v_d) \varphi(t) dt. \tag{52}$$

Temperature convection stabilization term This term can be treated in the same way that the velocity convection term (see [21, 22]). That is:

$$\begin{aligned} & \|\Pi_{h,2}^*(\tilde{\mathbf{u}}_h^- \cdot \nabla z_h)\|_{L^2(L^2)} \\ & \leq C \left(\|\tilde{\mathbf{u}}_h^-\|_{L^2(L^2)} \|\nabla(z_h - z)\|_{L^\infty} + \|\tilde{\mathbf{u}}_h^- - \mathbf{u}\|_{L^2(L^2)} \|\nabla z\|_{L^\infty} + \|(I - \Pi_{h,2})(\mathbf{u} \cdot \nabla z)\|_{L^2(L^2)} \right). \end{aligned}$$

Thus:

$$\lim_{(h, \Delta t) \rightarrow 0} \|\Pi_{h,2}^*(\tilde{\mathbf{u}}_h^- \cdot \nabla z_h)\|_{L^2(L^2)} = 0. \tag{53}$$

As:

$$\int_0^T S_h^{conv}(t) \varphi(t) dt \leq C h \|\varphi\|_{L^\infty(0,T)} \|\tilde{c}_h\|_{L^2(L^2_{\tau_2})} \|\Pi_{h,2}^*(\tilde{\mathbf{u}}_h^- \cdot \nabla z_h)\|_{L^2(L^2)},$$

using (27) and (53), we obtain:

$$\lim_{(h, \Delta t) \rightarrow 0} \int_0^T S_h^{conv}(t) \varphi(t) dt = 0.$$

Buoyancy stabilization term. As:

$$\begin{aligned} & \int_0^T S_h^{buo}(t) \varphi(t) dt \\ & \leq C h \lambda \|\varphi\|_{L^\infty(0,T)} \left(\|\Pi_{h,1}^*(\tilde{\mathbf{u}}_h^- \cdot \nabla v_{hd} + \partial_d q_h)\|_{L^2(L^2)} h \|\tilde{\theta}_h^-\|_{L^2(L^2)} + \|v_{hd}\|_{L^2} \|\tilde{c}_h\|_{L^2(L^2_{\tau_2})} \right), \end{aligned}$$

taking into account (27) and the fact that S_h^{mom} vanishes in the limit (see [21, 22]), we deduce:

$$\lim_{(h, \Delta t) \rightarrow 0} \int_0^T S_h^{buo}(t) \varphi(t) dt = 0.$$

This concludes the proof of convergence for method (14). For method (15) the proof is the same, changing in (51) the buoyancy term $c(\tilde{U}_h^-(t), \mathbf{V}_h)$ by $c(\tilde{U}_h(t), \mathbf{V}_h)$ and taking into account that (52) also holds for $\tilde{\theta}_h$. \square

Remark 4.11 The previous analysis allows to prove optimal convergence order for methods (14) and (15). Assuming an augmented regularity for the data and the solution of problem (2):

$$\begin{aligned} F &\in C^0(0, T; \mathbf{X}'), \partial_t F \in L^2(0, T; \mathbf{X}'), U_0 \in H^s(\Omega)^{d+1}, \\ U &\in C^0(0, T; H^{s+1}(\Omega)^{d+1}), \partial_{tt} U \in L^2(0, T; L^2(\Omega)^{d+1}), \\ P &\in C^0(0, T; H^s(\Omega)) \cap C^1(0, T; L^2(\Omega)); \end{aligned}$$

and assuming also that the discretization parameters h and Δt are small enough, then the following error estimate for a solution $\{U_h, p_h\}_{h>0}$ of (14) or (15) holds:

$$\|U - U_h\|_{l^\infty(\mathbf{L}^2)} + \sqrt{\mu} \|U - U_h\|_{l^2(X)} + \|P - P_h\|_{l^\infty(\mathbf{L}^2)} \leq C(h^s + \Delta t), \tag{54}$$

with C a positive constant independent of h and Δt and $2 \leq s \leq l$, where $l = m = n$ is the order of FE spaces (6). We are using the notation:

$$\begin{aligned} \|U - U_h\|_{l^\infty(\mathbf{L}^2)} &= \max_{n=1, \dots, N} \|U(\cdot, t_n) - U_h^n\|_{\mathbf{L}^2} \\ \|U - U_h\|_{l^2(X)} &= \left(\sum_{n=1}^N \Delta t \|U(\cdot, t_n) - U_h^n\|_X \right)^{1/2}. \end{aligned}$$

Thus, taking $s = l$ in (54), we deduce that for smooth flows the convergence of proposed methods is optimal with respect to the order of polynomial interpolation.

This error estimate is proved from the results obtained in [1] for a LPS discretization of the Navier–Stokes equations, using the techniques introduced therein to treat the buoyancy terms. We do not include the proof here for brevity.

5 Numerical Tests

In this section, we present some numerical tests to validate the performance of the proposed method solving natural convection problems. We consider the classical two-dimensional problem of a flow in a square cavity with differentially heated vertical walls and we compare our results with benchmark solutions in the literature.

More concretely, we solve problem (1) in the domain $\Omega = (0, 1)^2$ with data $\mathbf{f} = \mathbf{0}$, $Q = 0$, Prandtl number $Pr = 0.71$ (air) and Rayleigh number in the range $[10^3, 10^7]$. The equations depend on the initial conditions:

$$\mathbf{u}_0(\mathbf{x}) = \mathbf{1}, \quad \theta_0(\mathbf{x}) = 1 \quad \text{in } \Omega.$$

To generate the buoyancy-driven air flow, the vertical left and right walls of the domain are maintained at different temperatures and the horizontal walls are adiabatic, namely there is no heat transfer through these walls. We impose the following boundary conditions for $t > 0$:

$$\begin{aligned}
 & \mathbf{u} = \mathbf{0} \quad \text{on } \Gamma, \\
 & \theta = 1 \quad \text{for } x = 0, \quad 0 \leq y \leq 1, \\
 & \theta = 0 \quad \text{for } x = 1, \quad 0 \leq y \leq 1, \\
 & \frac{\partial \theta}{\partial y} = 0 \quad \text{for } y = 0, 1, \quad 0 \leq x \leq 1.
 \end{aligned}$$

We have numerically solved this problem with method (15). We choose as stabilization operator a Scott–Zhang-like interpolation operator, because of its efficiency and easy implementation. Also we use $P2$ FE for velocity, pressure, and temperature in space, and integrating in time until obtaining a steady solution. We have used uniform meshes with $h = \sqrt{2} \cdot 0.02$ for $Ra = 10^3$ and $Ra = 10^4$, and $h = \sqrt{2} \cdot 0.0125$ for higher Ra values ($Ra \geq 10^5$). All computations have been performed with the FreeFem++ software (Cf. [35]). Note that to reach a stable steady state with model (15) for the highest Rayleigh numbers, a rather small time step has to be used, as suggested by Theorem 4.8. A time step $\Delta t = 6.25 \cdot 10^{-5}$ has been used for instance to compute the discrete solution at $Ra = 10^7$.

Contours lines for final horizontal and vertical velocities, final temperature and pressure for different Rayleigh numbers are plotted in Figs. 1, 2, 3, 4 and 5. We can see that for lower Rayleigh numbers, Figs. 1 and 2, there is a dominant recirculating motion in the core of the region. Two eddies, for horizontal and vertical velocities can be observed. For higher Rayleigh numbers, Figs. 3, 4 and 5, these eddies are stretched to top left and bottom right corners for horizontal velocity, and similarly become closer to the hot and cold walls for vertical velocity. Isotherms also reveal the different regimes of the flow respect to Rayleigh number. At the lowest Rayleigh numbers, the temperature is almost linear with vertical contours and the heat transfer is primarily in form of conduction. However, as the Rayleigh number increases, temperature convection becomes prominent. The isotherms gradually transforms

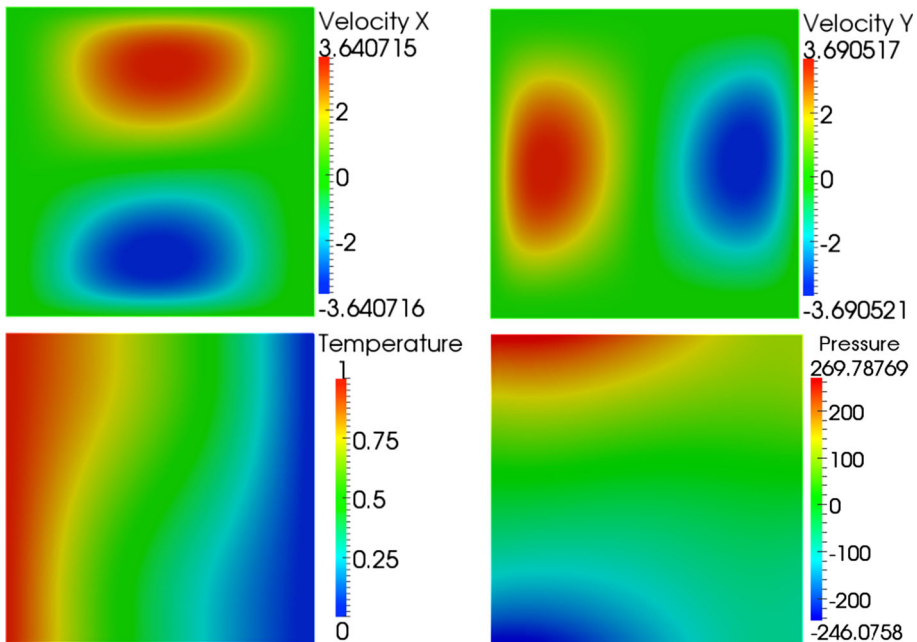


Fig. 1 Contours lines for horizontal and vertical velocity, temperature and pressure for $Ra = 10^3$

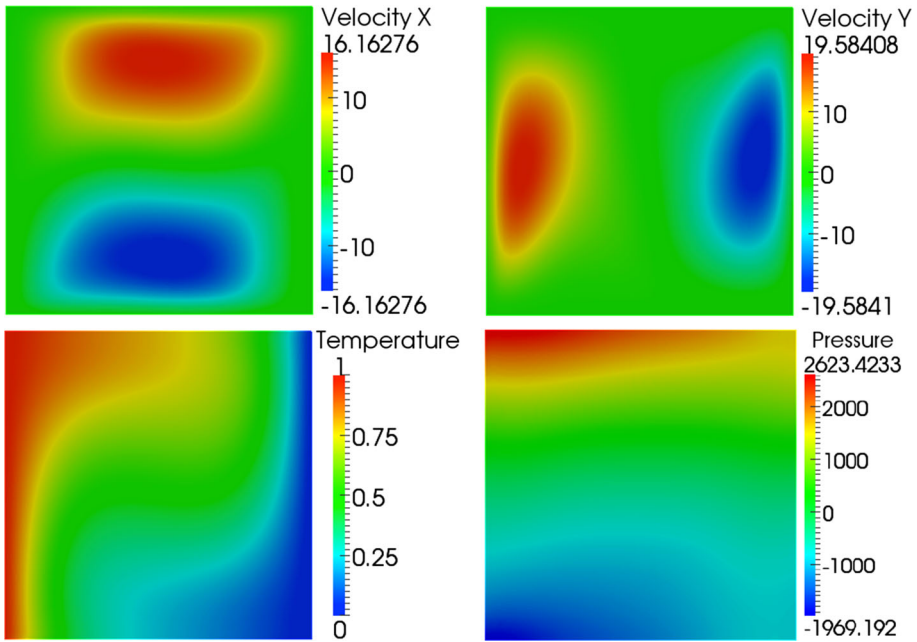


Fig. 2 Contours lines for horizontal and vertical velocity, temperature and pressure for $Ra = 10^4$

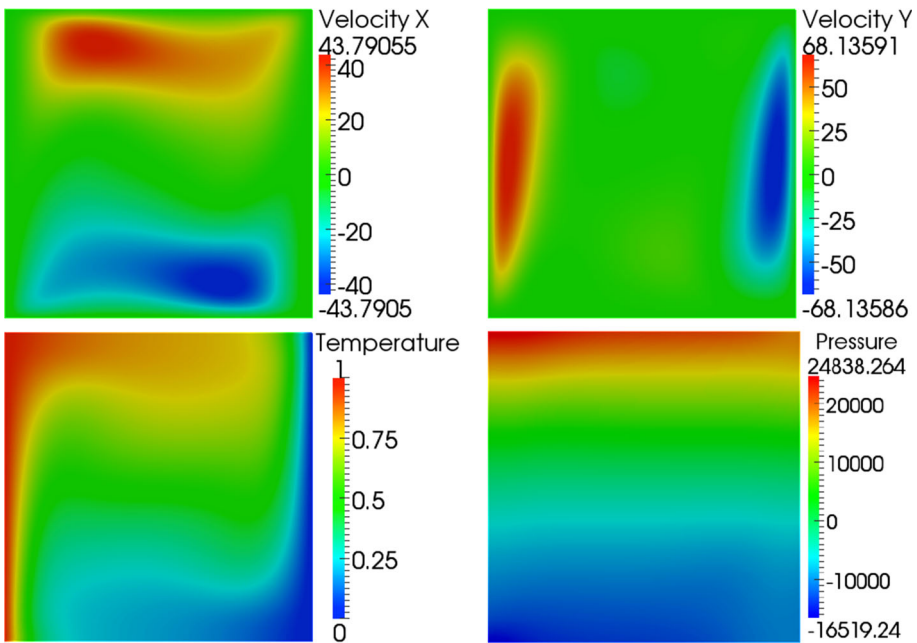


Fig. 3 Contours lines for horizontal and vertical velocity, temperature and pressure for $Ra = 10^5$

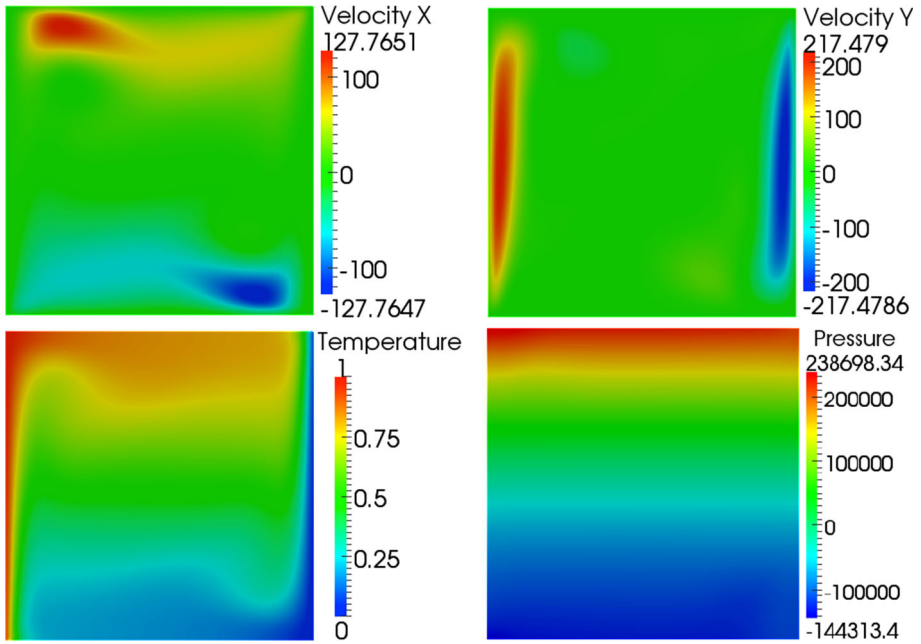


Fig. 4 Contours lines for horizontal and vertical velocity, temperature and pressure for $Ra = 10^6$

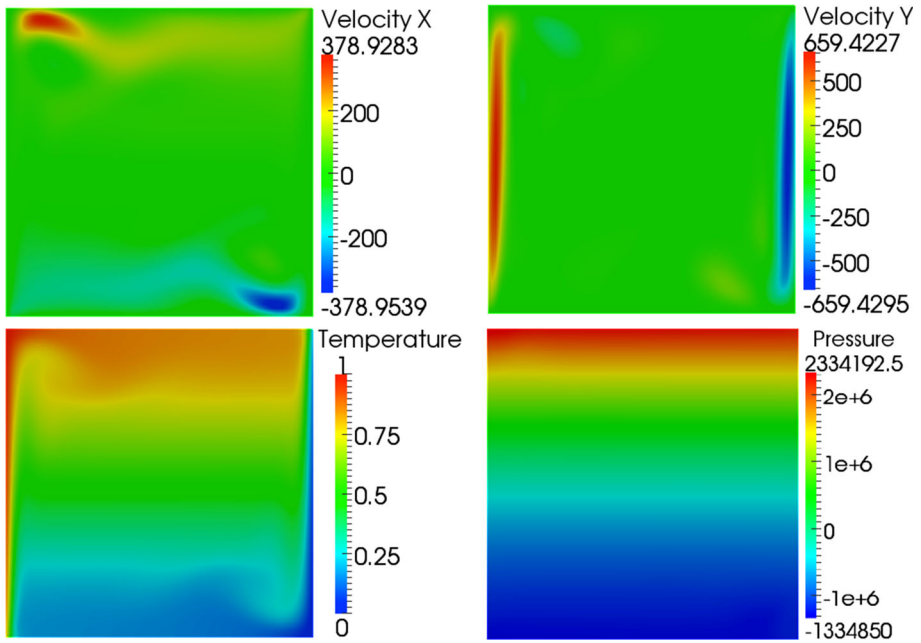


Fig. 5 Contours lines for horizontal and vertical velocity, temperature and pressure for $Ra = 10^7$

Table 1 Comparison of average Nusselt number

Ra	Cf. [31]	Cf. [43]	Cf. [42]	Cf. [53]	Cf. [10]	LPS
10^3	1.118	1.117	1.074	1.117	1.112	1.118
10^4	2.243	2.243	2.084	2.254	2.198	2.245
10^5	4.519	4.521	4.300	4.598	4.465	4.524
10^6	8.800	8.806	8.743	8.976	8.783	8.852
10^7	–	16.400	13.99	16.656	16.46	16.789

into horizontal except for the immediate neighborhood of the hot and cold walls, where remain parallel to the isothermal vertical walls. For $Ra \geq 10^5$, the warmer air is transported to the cold wall and a boundary layer near the vertical walls grows. This qualitative behavior of the solution agrees with the benchmark solution given in [31].

To validate the solution also from the quantitative point of view, we measure the heat rate convected from the wall to the fluid. To do so, we consider the local heat flux in the horizontal direction given by the Nusselt number:

$$Nu := u \theta - \frac{\partial \theta}{\partial x},$$

where u is the horizontal component of the velocity, and we compute the average Nusselt number in the whole cavity:

$$\overline{Nu} = \int_0^1 \int_0^1 Nu(x, y) dy dx.$$

Table 1 shows the average Nusselt numbers computed for different Rayleigh numbers. In this table, we can compare the results obtained from our solution (LPS) together with those obtained in other research works and this enables to conclude that the results are very similar. We remark that these results are obtained with a relatively coarse uniform grid at the highest Rayleigh numbers, which is for instance more than two times coarser the one used in [10] that is in addition refined near the vertical walls.

6 Conclusions

In the present work, a local projection stabilization (LPS) method for numerical discretization of the Boussinesq–Navier–Stokes equations as a model for natural convection is introduced. The method is derived from the variational multi-scale (VMS) formalism, by retaining, in addition to the dissipative interactions, the crossed interactions between resolved and sub-scales of momentum and temperature, to model the buoyancy interactions between these scales.

We have proved the well posedness of the new method in $L^\infty(\mathbf{L}^2) \cap L^2(\mathbf{H}^1)$. The new crossed terms modeling sub-grid to velocity–temperature interactions are controlled by means of the L^2 estimates of velocity and temperature, so as the estimates of the dissipative stabilization terms. The obtained stability estimates allow to pass to the weak limit in the evolution problem.

We present numerical tests for the 2D motion of a fluid in a square cavity whose vertical walls are maintained at different temperatures on relatively coarse grids. Numerical results by

comparison with reference solutions show the ability of the proposed method for accurately simulating high Rayleigh number flows with relatively coarse grids.

In the authors opinion, the work performed in this paper confirms on one hand the ability of the LPS method by interpolation to solve fluid flows with relatively low computational cost and high accuracy. On another hand, the numerical analysis performed to handle the terms modeling the interactions between resolved scales and sub-scales of velocity and temperature could open new doors for the analysis (not available in the current literature) of fully residual-based VMS turbulence models, where cross terms coupling all the residual appear. This study is today in progress.

Acknowledgements Research partially supported by Junta de Andalucía Excellence Project P12-FQM-454. Samuele Rubino would also gratefully acknowledge the financial support received from ERC Project H2020-EU.1.1.-639227, IdEx Bordeaux (Excellence Initiative of Université de Bordeaux) and FSMP (Fondation Sciences Mathématiques de Paris) during his postdoctoral research involved in this article.

References

- Ahmed, N., Chacón Rebollo, T., John, V., Rubino, S.: Analysis of a full space–time discretization of the Navier–Stokes equations by a local projection stabilization method. *IMA J. Numer. Anal.* (2016). doi:[10.1093/imanum/drw048](https://doi.org/10.1093/imanum/drw048)
- Ahmed, N., Chacón Rebollo, T., John, V., Rubino, S.: A review of variational multiscale methods for the simulation of turbulent incompressible flows. *Arch. Comput. Methods Eng.* **24**, 115–164 (2017)
- Ahmed, N., Matthies, G., Tobiska, L., Xie, H.: Discontinuous Galerkin time stepping with local projection stabilization for transient convection–diffusion–reaction problems. *Comput. Methods Appl. Mech. Eng.* **200**(21–22), 1747–1756 (2011)
- Arndt, D., Dallmann, H., Lube, G.: Local projection FEM stabilization for the time-dependent incompressible Navier–Stokes problem. *Numer. Methods Partial Differ. Equ.* **31**(4), 1224–1250 (2015)
- Barrenechea, G., Valentin, F.: Consistent local projection stabilized finite element methods. *SIAM J. Numer. Anal.* **48**(5), 1801–1825 (2010)
- Barrenechea, G.R., John, V., Knobloch, P.: A local projection stabilization finite element method with nonlinear crosswind diffusion for convection–diffusion–reaction equations. *ESAIM Math. Model. Numer. Anal.* **47**(5), 1335–1366 (2013)
- Bazilevs, Y., Calo, V.M., Cottrell, J.A., Hughes, T.J.R., Reali, A., Scovazzi, G.: Variational multiscale residual-based turbulence modeling for large eddy simulation of incompressible flows. *Comput. Methods Appl. Mech. Eng.* **197**(1–4), 173–201 (2007)
- Becker, R., Braack, M.: A finite element pressure gradient stabilization for the Stokes equations based on local projections. *Calcolo* **38**(4), 173–199 (2001)
- Becker, R., Braack, M.: A two-level stabilization scheme for the Navier–Stokes equations. In: *Numerical Mathematics and Advanced Applications*, pp. 123–130. Springer (2004)
- Benítez, M., Bermúdez, A.: A second order characteristics finite element scheme for natural convection problems. *J. Comput. Appl. Math.* **235**(11), 3270–3284 (2011)
- Bernard, J.M.: Density results in sobolev spaces whose elements vanish on a part of the boundary. *Chin. Ann. Math.* **B 32**, 823–846 (2011)
- Bernardi, C., Maday, Y., Rapetti, F.: *Discrétisations variationnelles de problèmes aux limites elliptiques*. Springer, Berlin (2004)
- Boland, J., Layton, W.: An analysis of the finite element method for natural convection problems. *Numer. Methods Partial Differ. Equ.* **6**(2), 115–126 (1990)
- Boland, J., Layton, W.: Error analysis for finite element methods for steady natural convection problems. *Numer. Funct. Anal. Optim.* **11**(5–6), 449–483 (1990)
- Braack, M., Burman, E.: Local projection stabilization for the Oseen problem and its interpretation as a variational multiscale method. *SIAM J. Numer. Anal.* **43**(6), 2544–2566 (2006)
- Braack, M., Burman, E., John, V., Lube, G.: Stabilized finite element methods for the generalized Oseen problem. *Comput. Methods Appl. Mech. Eng.* **196**(4–6), 853–866 (2007)
- Burman, E., Fernández, M.A.: Continuous interior penalty finite element method for the time-dependent Navier–Stokes equations: space discretization and convergence. *Numer. Math.* **107**(1), 39–77 (2007)

18. Chacón Rebollo, T.: A term by term stabilization algorithm for finite element solution of incompressible flow problems. *Numer. Math.* **79**(2), 283–319 (1998)
19. Chacón Rebollo, T., Gómez Mármol, M., Girault, V., Sánchez Muñoz, I.: A high order term-by-term stabilization solver for incompressible flow problems. *IMA J. Numer. Anal.* **33**(3), 974–1007 (2013)
20. Chacón Rebollo, T., Gómez Mármol, M., Girault, V., Sánchez Muñoz, I.: A reduced discrete inf–sup condition in L^p for incompressible flows and application. *M2AN* **49**(4), 1219–1238 (2015)
21. Chacón Rebollo, T., Gómez Mármol, M., Restelli, M.: Numerical analysis of penalty stabilized finite element discretizations of evolution Navier–Stokes equation. *J. Sci. Comput.* **61**(1), 1–28 (2014)
22. Chacón Rebollo, T., Gómez Mármol, M., Rubino, S.: Finite element approximation of an unsteady projection-based VMS turbulence model with wall laws. In: Knobloch, P. (ed.) *Boundary and Interior Layers, Computational and Asymptotic Methods—BAIL 2014*, volume 108 of *Lecture Notes in Computational Science and Engineering*, pp. 47–73. Springer, Berlin (2015)
23. Chacón Rebollo, T., Gómez Mármol, M., Rubino, S.: Numerical analysis of a finite element projection-based VMS turbulence model with wall laws. *Comput. Methods Appl. Mech. Eng.* **285**, 379–405 (2015)
24. Chacón Rebollo, T., Hecht, F., Gómez Mármol, M., Orzetti, G., Rubino, S.: Numerical approximation of the Smagorinsky turbulence model applied to the primitive equations of the ocean. *Math. Comput. Simul.* **99**, 54–70 (2014)
25. Chacón Rebollo, T., Lewandowski, R.: *Mathematical and Numerical Foundations of Turbulence Models and Applications*. Birkhäuser, Basel (2014)
26. Çibik, A., Kaya, S.: A projection-based stabilized finite element method for steady-state natural convection problem. *J. Math. Anal. Appl.* **381**(2), 469–484 (2011)
27. Codina, R., Principe, J.: Dynamic subscales in the finite element approximation of thermally coupled incompressible flows. *Int. J. Numer. Methods Fluids* **54**(6–8), 707–730 (2007)
28. Codina, R., Principe, J., Avila, M.: Finite element approximation of turbulent thermally coupled incompressible flows with numerical sub-grid scale modelling. *Int. J. Numer. Methods Heat Fluid Flow* **20**(5), 492–516 (2010)
29. Codina, R., Principe, J., Guasch, O., Badia, S.: Time dependent subscales in the stabilized finite element approximation of incompressible flow problems. *Comput. Methods Appl. Mech. Eng.* **196**(21–24), 2413–2430 (2007)
30. Dallmann, H., Arndt, D., Lube, G.: Local projection stabilization for the Oseen problem. *IMA J. Numer. Anal.* **36**(2), 796–823 (2016)
31. de Vahl Davis, G.: Natural convection of air in a square cavity: a benchmark numerical solution. *Int. J. Numer. Methods Fluids* **3**, 249–264 (1983)
32. Galdi, G.P.: An introduction to the Navier–Stokes initial-boundary value problems. In: *Fundamental Directions in Mathematical Fluid Mechanics. Advances in Mathematical Fluid Mechanics*, pp. 1–70. Birkhäuser, Basel (2000)
33. Gresho, P.M., Lee, R.L., Chan, S.T., Sani, R.L.: Solution of the time-dependent incompressible Navier–Stokes and Boussinesq equations using the Galerkin finite element method. In: *Approximation Methods for Navier–Stokes problems (Proceedings of Symposium, University of Paderborn, Paderborn, 1979)*, volume 771 of *Lecture Notes in Mathematics*, pp. 203–222. Springer, Berlin (1980)
34. He, L., Tobiska, L.: The two-level local projection type stabilization as an enriched one-level approach. *Adv. Comput. Math.* **36**(4), 503–523 (2012)
35. Hecht, F.: New development in FreeFem++ (www.freefem.org). *J. Numer. Math.* **20**(3–4), 251–265 (2012)
36. Horgan, C.O.: Korn’s inequalities and their applications in continuum mechanics. *SIAM Rev.* **37**(4), 491–511 (1995)
37. Hughes, T.J.R., Feijóo, G.R., Mazzei, L., Quincy, J.-B.: The variational multiscale method—a paradigm for computational mechanics. *Comput. Methods Appl. Mech. Eng.* **166**(1–2), 3–24 (1998)
38. Knobloch, P.: A generalization of the local projection stabilization for convection–diffusion–reaction equations. *SIAM J. Numer. Anal.* **48**(2), 659–680 (2010)
39. Knobloch, P., Lube, G.: Local projection stabilization for advection–diffusion–reaction problems: one-level vs. two-level approach. *Appl. Numer. Math.* **59**(12), 2891–2907 (2009)
40. Landau, L., Lifshitz, E.: *Fluid Mechanics. Course of Theoretical Physics*, vol. 6. Pergamon, Oxford (1982)
41. Löwe, J., Lube, G.: A projection-based variational multiscale method for large-eddy simulation with application to non-isothermal free convection problems. *Math. Models Methods Appl. Sci.* **22**(2), 1150011 (2012)
42. Manzari, M.: An explicit finite element algorithm for convective heat transfer problems. *Int. J. Numer. Methods Heat Fluid Flow* **9**, 860–877 (1999)
43. Massarotti, N., Nithiarasu, P., Zienkiewicz, O.: Characteristic-based-split (CBS) algorithm for incompressible flow problems with heat transfer. *Int. J. Numer. Methods Heat Fluid Flow* **8**, 969–990 (1998)

44. Matthies, G., Skrzypacz, P., Tobiska, L.: A unified convergence analysis for local projection stabilisations applied to the Oseen problem. *M2AN Math. Model. Numer. Anal.* **41**(4), 713–742 (2007)
45. Matthies, G., Skrzypacz, P., Tobiska, L.: Stabilization of local projection type applied to convection–diffusion problems with mixed boundary conditions. *Electron. Trans. Numer. Anal.* **32**, 90–105 (2008)
46. Matthies, G., Tobiska, L.: Local projection type stabilization applied to inf-sup stable discretizations of the Oseen problem. *IMA J. Numer. Anal.* **35**(1), 239–269 (2015)
47. Rabinowitz, P.H.: Existence and nonuniqueness of rectangular solutions of the Bénard problem. *Arch. Ration. Mech. Anal.* **29**, 32–57 (1968)
48. Roos, H.-G., Stynes, M., Tobiska, L.: Robust Numerical Methods for Singularly Perturbed Differential Equations. Convection–Diffusion–Reaction and Flow Problems, volume 24 of Springer Series in Computational Mathematics, 2nd edn. Springer-Verlag, Berlin (2008)
49. Rubino, S.: Numerical Modeling of Turbulence by Richardson Number-Based and VMS Models. Ph.D. thesis, Univeristy of Seville (2014)
50. Schlichting, H., Gertesten, K.: Boundary Layer Theory. Springer, Berlin (2004)
51. Simon, J.: Compact sets in $L^p(0, T; B)$. *Annali Mat. Pura Applicata (IV)* **146**, 65–96 (1987)
52. Tobiska, L., Winkel, C.: The two-level local projection type stabilization as an enriched one-level approach. A one-dimensional study. *Int. J. Numer. Anal. Model.* **7**(3), 520–534 (2010)
53. Wan, D., Patnaik, B., Wei, G.: A new benchmark quality solution for the buoyancy-driven cavity by discrete singular convolution. *Numer. Heat Transf.* **40**, 199–228 (2001)
54. Zhang, Y., Hou, Y., Zhao, J.: Error analysis of a fully discrete finite element variational multiscale method for the natural convection problem. *Comput. Math. Appl.* **68**(4), 543–567 (2014)